Cell Reports

Article

The lifespan evolution of individualized neurophysiological traits

Graphical abstract

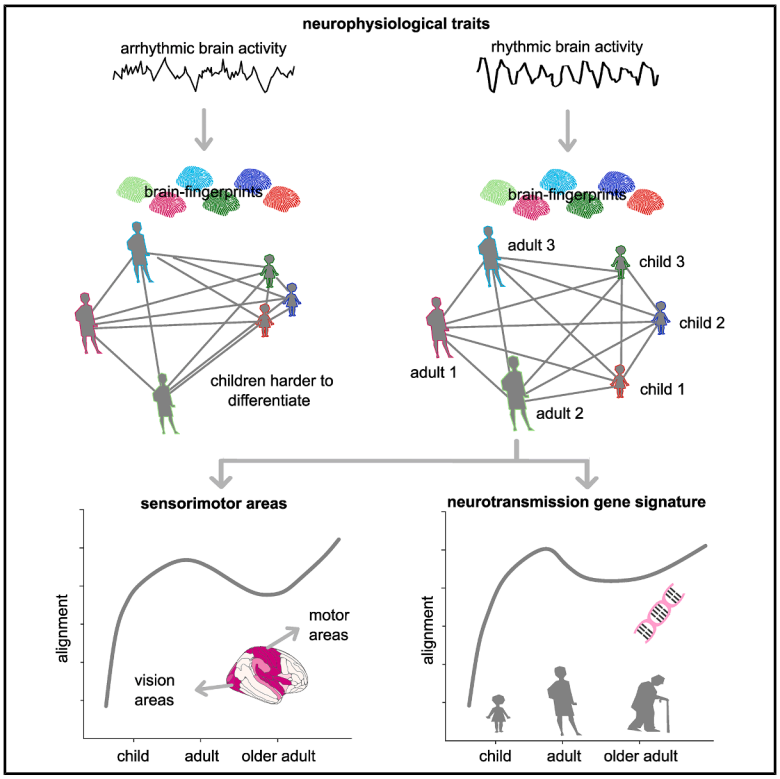

Highlights

- This study examines the development of individualized brain activity across a person's life
- Rhythmic neurophysiological traits can accurately differentiate children and adults
- Sensory and motor regions become increasingly distinctive in early adulthood
- Neurodevelopmental changes in differentiable brain activity align with gene expression

Authors

Jason da Silva Castanheira, Alex I. Wiesman, Margot J. Taylor, Sylvain Baillet

Correspondence

sylvain.baillet@mcgill.ca

In brief

da Silva Castanheiro et al. examine the development of individualized brain activity across a person's life. Rhythmic brain activity distinguishes individuals across age groups, with activity in sensory and motor regions becoming increasingly distinctive in early adulthood. These developmental changes in individualized brain activity align with specific patterns of cortical gene expression.

da Silva Castanheira et al., 2025, Cell Reports *44*, 116657
December 23, 2025
https://doi.org/10.1016/j.celrep.2025.116657

CellPress

Cell Reports

CellPress
OPEN ACCESS

Article

The lifespan evolution of individualized neurophysiological traits

Jason da Silva Castanheira,[1,2] Alex I. Wiesman,[3] Margot J. Taylor,[4,5,6] and Sylvain Baillet[1,2,7,8,9,*]
[1]Montreal Neurological Institute, McGill University, Montreal, QC, Canada
[2]Department of Experimental Psychology and Institute for Cognitive Neuroscience, University College London, 17-19 Alexandra House, London WC1N 3AZ, UK
[3]Department of Biomedical Physiology & Kinesiology, Simon Fraser University, Burnaby, BC, Canada
[4]Diagnostic and Interventional Radiology, Hospital for Sick Children, Toronto, ON, Canada
[5]Neurosciences & Mental Health, Research Institute, The Hospital for Sick Children, Toronto, ON, Canada
[6]Departments of Psychology and Medical Imaging, University of Toronto, Toronto, ON, Canada
[7]Centre de Recherche du Centre Hospitalier de l'Université de Montréal (CRCHUM), Montreal, QC, Canada
[8]Department of Neuroscience, University of Montreal, Montreal, QC, Canada
[9]Lead contact
*Correspondence: sylvain.baillet@mcgill.ca
https://doi.org/10.1016/j.celrep.2025.116657

SUMMARY

How do neurophysiological traits that characterize individuals evolve across the lifespan? To address this question, we analyzed task-free magnetoencephalographic recordings from over 1,000 individuals aged 4–89. We found that neurophysiological activity is more similar between individuals in childhood than in adulthood, an effect driven predominantly by arrhythmic brain activity. In contrast, periodic activity-based profiles remain reliable markers of individuality across all ages. The cortical regions most critical for determining individuality shift across neurodevelopment and aging, with sensorimotor cortices becoming increasingly prominent in adulthood. These developmental changes in neurophysiology align closely with the expression of cortical genetic systems related to ion transport and neurotransmission, suggesting a growing influence of genetic factors on neurophysiological traits across the lifespan. Notably, this alignment is strongest in late adolescence, a critical period when genetic factors significantly shape brain individuality. Overall, our findings advance our understanding of the evolving biological foundations of inter-individual differences.

INTRODUCTION

The neurophysiological mechanisms underlying individuality in behavioral traits are a cornerstone of both basic and clinical neuroscience.[1–8] Beyond anatomical differences, functional neuroimaging studies have demonstrated that patterns of brain activity and connectivity reliably differentiate individuals.[9–12] These neurophysiological traits, referred to as "brain fingerprints" in the literature, are associated with cognitive abilities[10,11,13,14] and various clinical conditions, including neurological and psychiatric disorders.[15–18] Moreover, these traits are heritable and linked to cortical gene expression.[19] Yet, the evolution of these individual-specific neurophysiological traits over the lifespan—amid extensive neurodevelopmental and aging-related brain changes—remains largely unexplored.

A wealth of neuroimaging research has documented nonlinear age-related changes in both brain structure and function, offering insights into lifespan development. Structurally, cortical thinning is a hallmark of aging, occurring progressively over time.[20–23] This thinning is particularly pronounced in higher-order association areas along the transmodal ends of the unimodal-to-transmodal functional gradient. Transmodal regions—associated with complex, integrative cognitive processes—show the earliest and most substantial reductions in cortical thickness.[24,25]

In terms of function, neurophysiological activity can be mapped using magnetoencephalography (MEG), which captures both periodic (oscillatory) and aperiodic (background) components of brain activity.[26,27] Periodic oscillations in different frequency bands (e.g., delta, theta, alpha, beta, and gamma) vary across individuals and systematically change with age. For instance, posterior dominant rhythms develop from slower (3–5 Hz) frequencies in early childhood to 6–7 Hz by 12 months and then into the alpha rhythm (8–13 Hz) characteristic of adults.[28–31] This rhythm slows again in older age, reflecting functional decline.[32–36] Aperiodic components, which reflect the dynamic balance of excitatory and inhibitory processes,[26,27,37–39] also evolve across the lifespan and are associated with age-related decline in sensory and cognitive functions.[36,40–44]

These structural and functional transformations underscore the complex interplay between neurophysiological and anatomical changes over time and offer insights into inter-individual differences in brain function and structure at the population level. This previous work affords researchers age-matched norms of a particular trait (for example, hippocampal volume) to which any individual can be compared.[20,30,45] This differs from the

brain fingerprinting approach, where researchers describe individual-specific neurophysiological traits that are stable within a person and can distinguish between individuals.

While behavioral traits and cognitive abilities evolve significantly across neurodevelopment and aging, it remains an open question whether the neurophysiological processes differentiating individuals exhibit similar degrees of transformation or maintain stability.

Previous studies have examined whether brain fingerprints remain differentiable across development using functional connectomes (FCs) derived from functional magnetic resonance imaging (fMRI), which has yielded mixed results. Some studies suggest that inter-individual differences in FC become more pronounced with age,[17,46–48] consistent with evidence of increasing genetic influence on cognition during development.[49–51] Others have found that infants and children can be differentiated as accurately as adults, suggesting early stability in individual FC traits[52–56] and seemingly in contrast to previous findings. Moreover, our previous work identified a cortical gene expression signature aligned to the neurophysiological traits of adults, which becomes increasingly expressed throughout neurodevelopment, hinting at potential developmental shifts in these traits. We are not aware of any previously published studies exploring whether neurophysiological traits derived from MEG in children are equally differentiable from those of adults.

Several factors may explain the disagreement as to whether individuals' brain activity becomes more differentiable with age, as observed in fMRI brain fingerprinting. Many previous studies have relied on task-based data, where children and adults may engage different cognitive strategies, complicating the separation of stable, trait-like patterns from transient, task-related states. This is particularly salient when task-evoked signals are regressed out from the blood-oxygen-level-dependent (BOLD) response to compute brain fingerprints, a correction that may not perform equally well across age groups. Residual task-related variance could therefore differentially bias fingerprinting results, especially if one demographic group engages with the task in a distinct manner. Resting-state acquisitions avoid this specific confound by not requiring removal of task-evoked signals, although they still capture a combination of intrinsic traits and momentary cognitive states.

Another explanation for this discrepancy may be age-dependent biases[57–59] in the hemodynamic response. While fMRI is an indirect measure of brain activity, MEG, on the other hand, directly measures neurophysiological signals, offering a clearer perspective on how differentiation of brain activity may evolve. Given the distinct biological origins of hemodynamic fMRI and electrophysiological MEG signals, it remains unknown whether neurophysiological traits become more individualized with age or whether consistent electrophysiological features differentiate individuals across development.

Emerging evidence also indicates that the brain regions most characteristic of healthy individuals differ significantly from those in clinical populations, where disease-related disruptions alter neurophysiological patterns.[15,16,60] This suggests that features critical for differentiation may shift in response to neural alterations due to disease or the cumulative effects of aging and development. Supporting this, models trained on young adult data to predict behavior from brain activity often fail to generalize when applied to older adults,[61,62] emphasizing the importance of age-specific patterns in studying individual differences.

This study addresses three objectives: (1) to determine whether the accuracy of individual differentiation based on MEG-derived neurophysiological traits changes with age, (2) to characterize how patterns of differentiation evolve across neurodevelopment and aging, and (3) to identify the brain regions most critical for differentiation and examine their alignment with cortical gradients of functional organization and gene expression.

Based on prior work in both developmental neuroimaging and MEG-derived neurophysiological traits, we advance three predictions. (1) Stability of differentiability: children will be differentiated as accurately from one another based on neurophysiological traits as adults, reflecting the early emergence of stable, individual-specific brain activity patterns. However, the regional features most critical for differentiation will vary across the lifespan. (2) Functional gradient alignment. Given evidence that the unimodal-to-transmodal gradient becomes increasingly important for functional organization throughout neurodevelopment,[24,25] we predict that salient features for participant differentiation will show progressively stronger alignment with this gradient from childhood to adulthood. (3) Genetic expression alignment. Building on our previous work linking adult neurophysiological traits to a cortical gene expression gradient enriched for neurotransmission and ion transport,[19] we predict that alignment with this genetic gradient will increase across neurodevelopment, reflecting maturational changes in the molecular processes supporting individual-specific brain activity.

In this study, we analyzed MEG-derived neurophysiological traits from a lifespan sample of 1,007 participants aged 4–89 years. We examined whether individuals could be differentiated across a wide age range and investigated how the topography of the most characteristic brain regions shifts with age. Our findings reveal that, while periodic brain activity reliably differentiates individuals across the lifespan, the regions contributing most strongly to this differentiation change systematically with age, aligning with cortical gradients of functional organization and gene expression. These results reconcile previous inconsistencies in the developmental trajectory of brain individuality and offer insights into how neurophysiological traits evolve throughout life.

RESULTS

We investigated three core aspects of neurophysiological traits across the lifespan. First, we evaluated whether individuals from different age groups, particularly children and older adults, could be accurately differentiated based on brief recordings of their neurophysiological brain activity. Next, we examined the ease with which we can differentiate individuals through neurodevelopment and aging. Finally, we assessed the spatial distribution of neurophysiological features that most strongly contribute to individual differentiation and analyzed how these features vary systematically with age and relate to established cortical gradients of functional organization and gene expression.

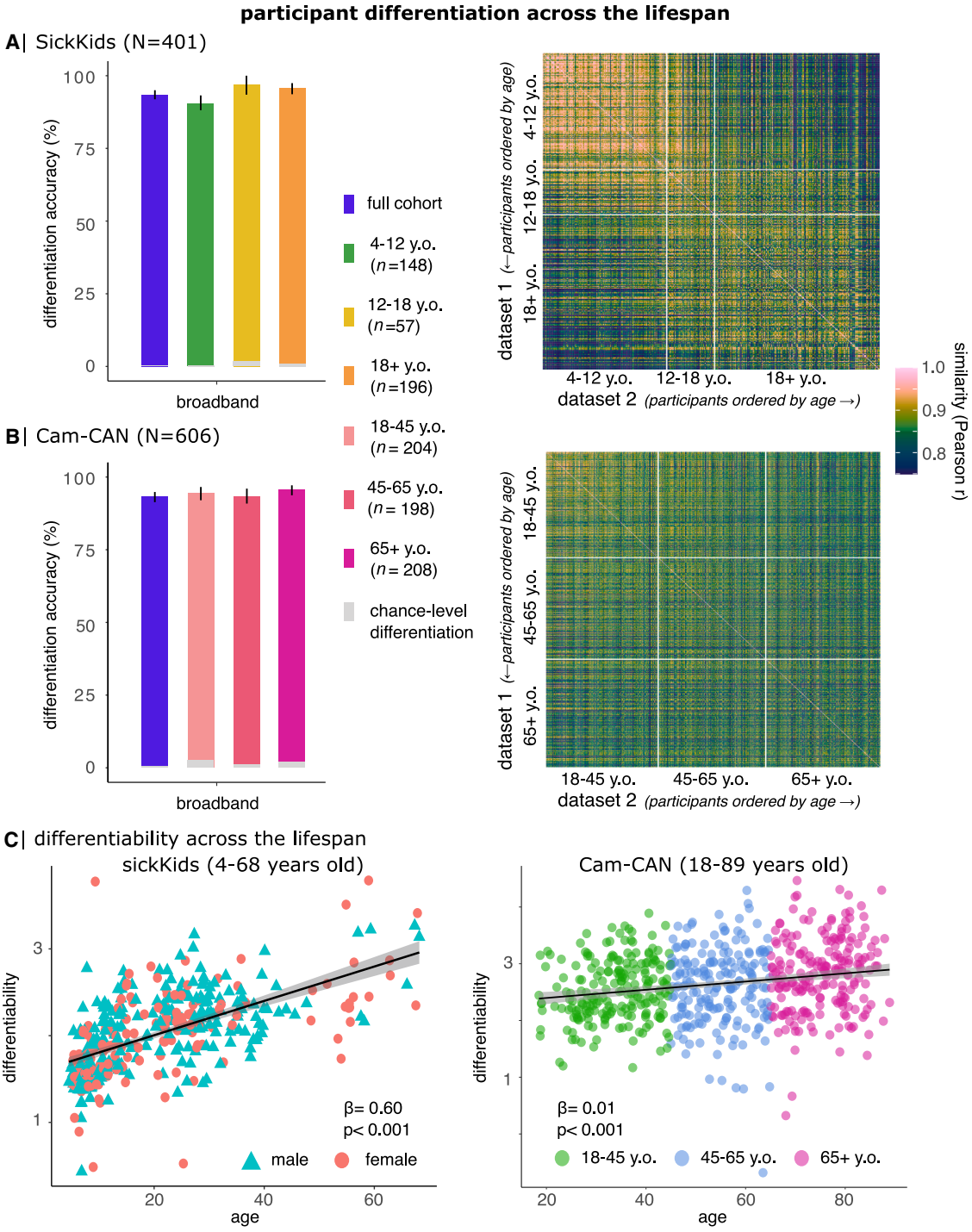

Figure 1. Age-related variations in neurophysiological differentiation accuracy

(A) Differentiation accuracy in the SickKids cohort (ages 4–68) using wide-band neurophysiological traits derived from 2-min MEG recordings. Gray bars at the base of the plot represent chance-level differentiation based on empty-room MEG recordings collected the same day as participants' sessions. Error bars denote bootstrapped 95% CIs. Right: similarity matrix illustrating self-similarity (diagonal) and other-similarity (off-diagonal) across two distinct data segments from each participant. Participants are ordered by ascending age; children (ages 4–12) exhibit higher other-similarity values, making differentiation more challenging.

(B) Differentiation accuracy in the Cam-CAN cohort (ages 18–89) using wide-band neurophysiological traits from 4-min MEG recordings. Gray bars represent chance-level differentiation as in (A). Error bars denote bootstrapped 95% CIs. Right: similarity matrix illustrating age-related changes in self- and other-similarity.

(legend continued on next page)

We used a neurophysiological trait differentiation method that replicates established brain-neurophysiological differentiation techniques.[9–11] This approach involved comparing each participant's neurophysiological traits—derived from one segment of data—with traits from all other participants, including a separate segment from the same individual. Correct differentiation was determined based on whether a participant's neurophysiological trait was more similar to their own trait (''self-similarity'') than to those of any other individual in the cohort (''other-similarity''). Differentiation accuracy was defined as the percentage of correctly differentiated participants across the cohort (STAR Methods). This analysis quantified differentiation accuracy across age groups and provided insights into the stability and uniqueness of neurophysiological traits over time.

Differentiation accuracy across age groups and neurophysiological components

We computed differentiation accuracy across four age cohorts from the SickKids dataset: (1) children aged 4–12 years (n = 148), (2) adolescents aged 12–18 years (n = 57), (3) adults aged 18–68 years (n = 196), and (4) all participants combined (n = 401).

Across all age groups, individuals were accurately differentiated with an overall accuracy of 93.4% (95% confidence interval [CI]: [91.9, 95.0]; Figure 1A). Differentiation accuracy for children was 90.3% (CI: [88.1, 93.2]), for adolescents 97.0% (CI: [93.5, 100.0]), and for adults 95.7% (CI: [93.6, 97.5]). These results were consistent when individual traits were derived from specific frequency bands and age-specific data subsets (Figures S1 and S7).

To investigate developmental trends, we assessed ''differentiability,''[9] a measure of how easily individuals could be differentiated based on their neurophysiological traits. We observed a strong positive linear relationship between age and differentiability (β = 0.60, SE = 0.04, 95% CI [0.52, 0.68], r^2 = 0.35, $p < 0.001$; Figure 1C). This increase was primarily driven by greater other-similarity in children, which made differentiation more challenging in this group. In contrast, adult traits exhibited lower similarity with other adults, enabling more accurate differentiation (Figure 1A, right). Self-similarity of neurophysiological traits did not scale with age in the SickKids cohort (r = −0.09, 95% CI [−0.18, 0.01], p = 0.07, Bayes Factor [BF] = 0.57).

To explore which age groups may be driving this effect, we conducted an exploratory analysis where we ran the same linear regression model restricted to participants below 40 years old and progressively increased the lower age cutoff from 4 years upward. The goal of this analysis was to determine at which cutoff the age-differentiation relationship became non-significant. We observed that, with a lower cutoff of 13 years, the age-differentiation relationship in the SickKids cohort for participants between the ages of 14 and 40 was non-significant (β = 0.09, p = 0.24). This result is consistent with the weaker age-differentiation relationship observed in the Cam-CAN cohort (see Differentiation accuracy and stability in older adults) and reinforces the interpretation that participants below the age of 13 are more challenging to differentiate from one another based on broadband neurophysiological traits.

To further explore the contributions of periodic and aperiodic components to differentiation, we decomposed the power spectral density (PSD) of each MEG cortical source time series into these two components. These decomposed spectra were then used to define individual periodic and aperiodic spectral traits (STAR Methods).

When differentiation accuracy was computed using aperiodic traits, accuracy dropped to 79.4% overall (CI: [76.6, 81.2]), with 75.8% accuracy for children (CI: [72.0, 79.6]), 86.5% for adolescents (CI: [80.4, 93.5]), and 84.5% for adults (CI: [80.9, 87.8]; Figure S7). In contrast, differentiation based on periodic traits remained highly accurate across all age groups, achieving 96.6% overall accuracy (CI: [95.3, 97.8]), 97.0% for children (CI: [95.7, 99.2]), 97.5% for adolescents (CI: [95.6, 100.0]), and 96.7% for adults (CI: [94.9, 98.7]; Figure S8).

Differentiation accuracy and stability in older adults

To extend our findings to older populations, we analyzed neurophysiological differentiation in an adult cohort (ages 18–89 years, n = 606) from the Cambridge Center for Aging Neuroscience (Cam-CAN) dataset.[63] Participants were divided into three age groups: young adults (18–45 years, n = 204), middle-aged adults (45–65 years, n = 194), and older adults (65–89 years, n = 208).

For the entire Cam-CAN cohort, differentiation accuracy was 93.2% (CI: [91.3, 94.8]). Differentiation accuracy varied slightly across age groups: 94.4% (CI: [92.0, 96.6]) for young adults, 93.4% (CI: [90.8, 96.0]) for middle-aged adults, and 95.6% (CI: [93.7, 97.1]) for older adults (Figure 1B). These findings were robust across frequency bands and decomposition of periodic and aperiodic traits (Figures S1, S8, and S9). Note that the differentiation accuracy for adults in the SickKids dataset was similar to that for the young adults in the Cam-CAN cohort.

To assess whether the stability of individual traits changes with age, we analyzed variations in self-similarity across age groups. No significant linear relationship was observed between self-similarity and age (β = −4.50, SE = 2.45, 95% CI [−9.31, 0.31], r^2 = 0.006, p = 0.06). However, we observed a modest positive linear relationship between differentiability and age (linear regression model: β = 0.01, SE = 1.40 × 10^{-3}, 95% CI [0.00, 0.01], r^2 = 0.042, $p < 0.001$), explaining 4.2% of the total variance (Figure 1C).

When differentiation accuracy was computed using aperiodic traits in the Cam-CAN cohort, accuracy remained high, 92.6% overall (CI: [90.9, 94.2]), with 91.7% accuracy for young adults (CI: [88.6, 94.9]), 95.4% for middle-aged adults (CI: [93.7, 97.1]), and 94.4% for adults (CI: [92.6, 96.0]; Figure S7). Similarly, differentiation based on periodic traits remained highly accurate

Older adults exhibit higher distinctiveness in their neurophysiological traits, contributing to the modest positive relationship between differentiation and age (Figure S2).

(C) Relationship between age and differentiability. Left (SickKids): a strong positive linear relationship explains 36% of the variance; colors indicate biological sex. Right (Cam-CAN): a weaker positive relationship explains 4% of the variance; colors indicate age groups. Statistics obtained from linear regression models. The shaded grey area represents 95% CI.

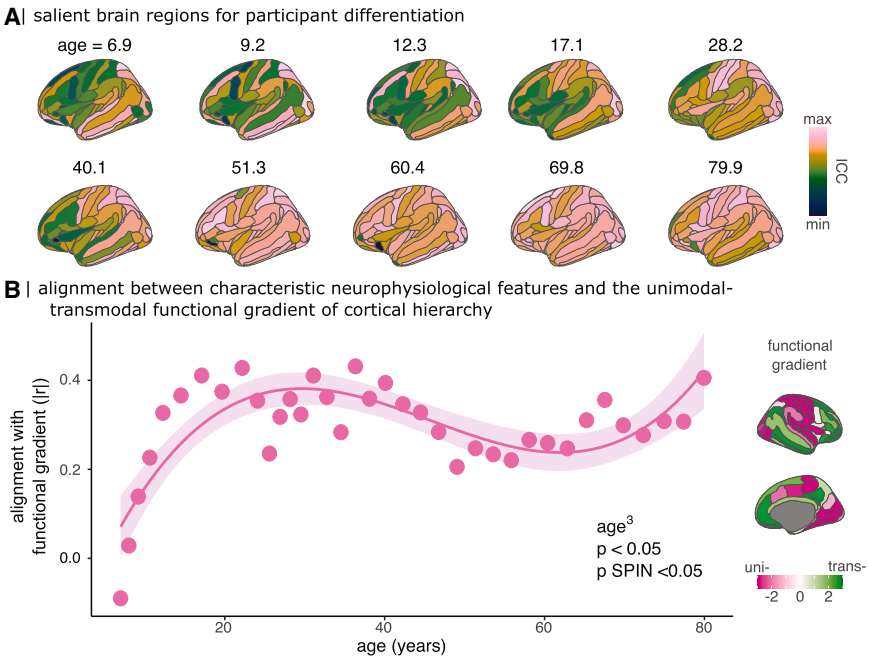

Figure 2. Sensorimotor brain regions become increasingly characteristic for individuals across the lifespan

(A) Topographic maps of intraclass correlation coefficients (ICCs) show the cortical regions that contribute most to individual neurophysiological differentiation across age groups (bins of ~100 individuals per map). Higher ICC values indicate cortical areas that play a significant role in distinguishing individuals within each age group. Sensorimotor regions become increasingly prominent with age.

(B) Scatterplot illustrating the alignment between characteristic cortical regions for participant differentiation (as shown in A) and the unimodal-to-transmodal functional gradient (inset on the right). The alignment exhibits a non-linear third-order polynomial trajectory across the lifespan, with weak alignment in early childhood that becomes stronger into young adulthood. We observed the strongest alignment at 36.3 years old. This highlights the evolving contribution of cortical regions to individual differentiation with age. The shaded area represents 95% CIs.

across all age groups, achieving 96.6% overall accuracy (CI: [95.1, 98.1]), 96.7% for young adults (CI: [93.7, 99.4]), 97.3% for middle-aged adults (CI: [96.6, 98.3]), and 97.6% for adults (CI: [96.6, 98.8]; Figure S8).

Age-related shifts in cortical regions influential for differentiation

Given the lower differentiation accuracy observed in children when using non-parameterized neurophysiological traits, we focused our analyses on periodic activity, which consistently demonstrated higher differentiation accuracy across all age groups.

Our primary goal was to identify the cortical regions most characteristic of individuals throughout the lifespan. We define "characteristic" regions as those where neurophysiological features most strongly contribute to individual differentiation. To quantify this, we used intraclass correlation coefficients (ICCs), which measure the consistency of neurophysiological features within individuals relative to variability across individuals.[9,10,16] High ICC values indicate that a specific neurophysiological feature is consistently similar within participants while being distinct across different participants. Regions with higher ICC values were deemed more influential for individual differentiation. To capture developmental trajectories, we used a sliding window approach to compute ICC maps across different age groups (STAR Methods).

Our findings revealed systematic shifts in the cortical regions most distinctive for individual differentiation over the lifespan. In children, lateral parietal and superior temporal regions were the most characteristic of individual differences. By early adulthood (ages 20–30 years), caudal and peri-central cortical regions emerged as the most distinctive, consistent with previous studies.[12,19] Across all age groups, orbitofrontal regions consistently contributed the least to differentiation (Figure 2A; Figures S9 and S10).

We examined how these characteristic cortical regions align with the unimodal-to-transmodal functional gradient,[64] a primary axis of neurodevelopment that reflects transitions from primary sensory motor areas to higher-order association cortices.[24,25] The alignment of characteristic regions with this gradient followed a non-linear trajectory across the lifespan (third-order polynomial: $\beta = -0.46$, SE = 0.07, 95% CI [−0.60, −0.31], $p < 0.001$, $p_{spin} = 0.00099$; Table S9). Alignment was weakest in early childhood (6.9 years old, r = 0.09, $p_{spin} = 0.26$) and strongest in early adulthood (36.3 years old, r = −0.44; Figure 2B), followed by 22.2 years old (r = −0.43), and 17.1 and 31.1 years old (r = −0.41). In older adults, the highest alignment was observed at 79.9 years old (r = −0.40). All observed alignments were negative, except for the earliest age group (6.9 years old), where we found a small positive alignment (r = 0.08), indicating maximal differentiation from transmodal regions. Negative alignments reflect maximal differentiation in unimodal (sensorimotor) regions, a pattern observed across most of the lifespan.

We tested age-related changes in the alignment between salient neurophysiological traits and the unimodal-to-transmodal functional gradient exclusively in the Cam-CAN sample. A significant non-linear trend emerged, with the weakest alignment observed in middle adulthood ($\beta = 0.34$, SE = 0.09, 95% CI [0.20, 0.48], $p < 0.001$, $p_{spin} = 0.000999$), an effect attenuated when considering the entire cohort (mean alignment of r = 0.28 for the entire sample between the ages of 40–65).

Despite the significant neurodevelopmental alignment of salient neurophysiological traits to the unimodal-to-transmodal gradient, we observed minimal alignment in childhood (mean age 9.2 years: r = −0.14, $p_{spin} = 0.25$; Figure 2B). This suggests that sensorimotor regions—which dominate adult differentiation—play a minimal role in childhood. Motivated by evidence that the motor-to-visual gradient is particularly relevant in early

development,[65] we tested its alignment in children and observed a significant effect (mean age 9.2 years: r = 0.43, $p_{spin} < 0.05$; Figure S11). This alignment did not vary significantly with age (third-order polynomial: $\beta = -0.24$, SE = 0.07, 95% CI [−0.38, −0.10], $p < 0.01$, $p_{spin} > 0.05$; Figure S11).

Alignment between neurophysiological differentiation and cortical gene expression across the lifespan

Previous research has shown that neurophysiological traits in adults align with a ventromedial-to-dorsolateral gene expression signature, involving genes associated with ion transport, synaptic functioning, and neurotransmitter release.[19] However, the evolution of this alignment across different developmental stages, particularly during critical periods of neurodevelopment, has remained unclear. We aimed to elucidate how the alignment between cortical neurophysiological traits and cortical gene expression changes across the lifespan (Figure 2A).

To investigate this relationship, we divided the gene differentiation signature into two sets: a positive set related to participant differentiation and a negative set associated with lower differentiation capabilities. The positive gene set primarily included processes related to ion transport, synaptic activity, and neurotransmitter release, while the negative set was linked to neurodevelopmental processes such as neurogenesis and cell morphogenesis.[19] This division allowed us to understand which gene expressions were related to neurophysiological differentiation across age groups (STAR Methods).

We first assessed whether the spatial organization of these gene sets remained stable across developmental stages, using data from the BrainSpan dataset,[66] which includes fetal through adult data. Consistent with prior findings indicating that the most pronounced changes in cortical gene expression occur prenatally,[67] the spatial distribution of the positive gene signature showed remarkable stability from infancy through childhood, adolescence, and adulthood (spatial correlations >0.71; Figure S12). In contrast, the negative gene signature exhibited weaker spatial consistency between childhood and adulthood (Figure S12). These results underscored the enduring relevance of the positive gene set for neurophysiological differentiation, prompting us to focus subsequent analyses on this gene group.

Next, we analyzed the alignment between cortical maps of neurophysiological differentiation and the positive gene signature. This alignment followed a third-order polynomial trajectory across the lifespan, with an initial increase, a midlife dip, and a subsequent rise. The strongest alignment was observed in late adolescence (17.1 years old; $\beta = 0.73$, SE = 0.11, 95% CI [0.51, 0.96], $p < 0.001$, $p_{spin} = 0.004$, $p_{permutation} = 0.001$; Table S12; Figure 3A). This finding suggests that adolescence represents a critical period during which neurophysiological features most strongly align with genetic signatures related to ion transport and neurotransmission,[19] likely reflecting a pivotal stage in the fine-tuning of neural circuits. Testing the non-linear relationship between age and the alignment of cortical maps of neurophysiological differentiation with the positive gene signature in only the Cam-CAN sample did not meet statistical significance after performing spatial autocorrelation-preserving permutations ($\beta = 0.26$, $p = 0.01$, $p_{spin} = 0.083$).

To gain deeper insights into how gene-neurophysiology alignment evolves, we conducted a partial least squares (PLS) analysis to examine the covariance between neurophysiological features and cortical gene expression data from the Allen Human Brain Atlas.[68] The analysis revealed significant covariance between cortical gene expression patterns and neurophysiological differentiation across the lifespan, particularly up to middle age (Figure 3B, left). Interestingly, the percentage of covariance explained by these latent components remained relatively stable across age groups (Figure 3B, middle), indicating that the relation between gene expression and neurophysiological differentiation is preserved over time. Additionally, gene loadings showed strong consistency across developmental stages, with Pearson correlations >0.75 between loadings from different age groups. This consistency suggests that the same gene signature drives neurophysiological differentiation throughout development (Figure 3B, right).

We further examined the contributions of specific neurophysiological frequency bands to the alignment with gene expression (Figure 3C). The relationship between periodic activity and gene expression varied significantly by frequency band and developmental stage. Theta band activity (4–8 Hz) showed a developmental shift in its relationship with cortical gene expression. In early development, theta traits were aligned with the negative gene expression pattern (6.9 years old, r = −0.43), but this relationship reversed later in life, with the strongest alignment with the positive gene set at 22.2 years old (r = 0.70). Alpha band activity (8–13 Hz) showed its strongest positive alignment at 12.3 years (r = 0.70), beta band traits (13–30 Hz) at 28.2 years (r = 0.60), and gamma traits (30–50 Hz) at 12.3 years (r = 0.55). These values represent the age bins with the highest observed correlations for each band (i.e., the point with the highest y value in the case of positive alignments in Figure 3C, highlighted with black outlines) and do not reflect the peak of the smoothed dotted lines.

Importantly, the smoothed dotted lines in Figure 3 depict trends rather than model-derived non-linear fits. Our aim with this analysis was to illustrate broad, frequency-specific developmental trajectories in the alignment between neurophysiological traits and gene expression across age. Across frequency bands, the data reveal distinct lifespan patterns; for example, theta-band activity shows early-life associations with the negative gene set before shifting toward strong positive alignment in adolescence and early adulthood. This pattern suggests that the specific contributions of different frequency bands to gene-neurophysiology covariance evolve dynamically across development.

These findings highlight the dynamic, frequency-specific nature of the molecular-genetic mechanisms underlying neurophysiological individuality. While the overarching genetic gradient remains consistent, the specific contributions of different frequency bands evolve across the lifespan, with greater alignment to genes related to neurogenesis and cell morphology earlier in development and greater alignment to genes related to neurotransmission in adulthood.[19]

Sensitivity analyses

We conducted sensitivity analyses to rule out potential confounding effects from environmental or physiological artifacts in both cohorts.

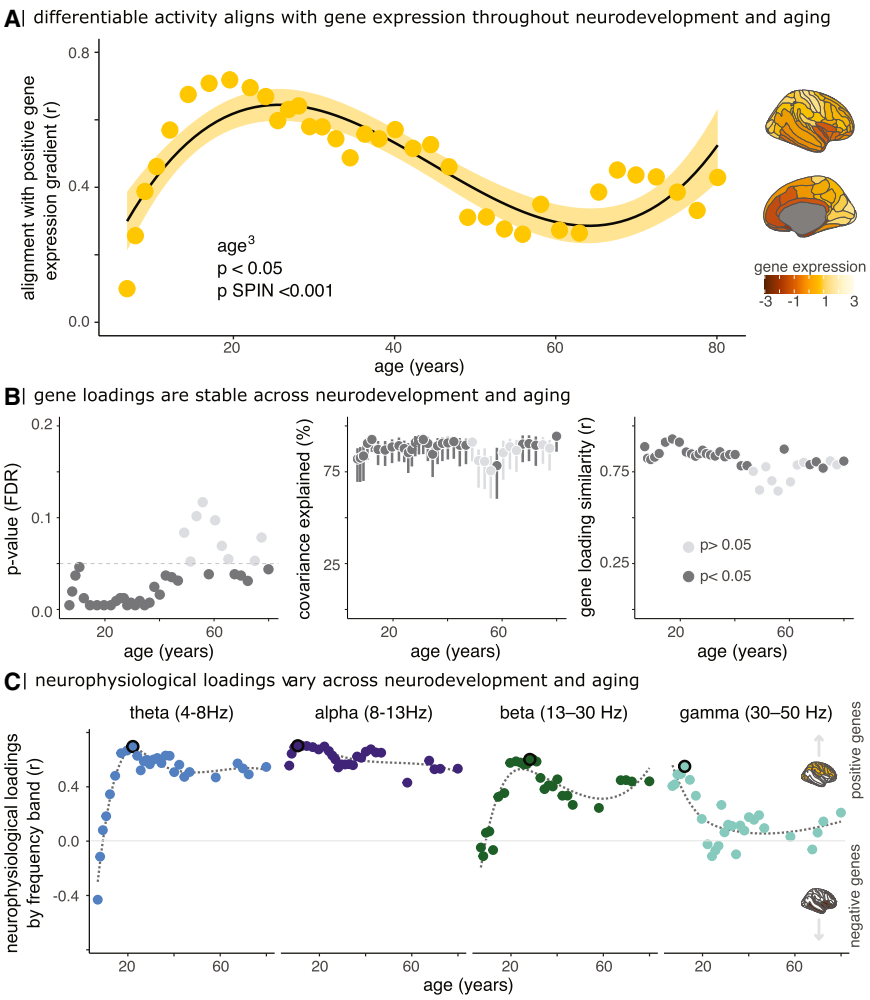

Figure 3. Lifespan variations in the alignment between gene expression and characteristic patterns of neurophysiological activity

(A) Cortical alignment between the positive gene expression signature and differentiable brain regions. The right inset shows the spatial distribution of the positive gene expression signature across the cortex. The graph illustrates the non-linear third-order polynomial alignment of this genetic signature with cortical regions most critical for neurophysiological differentiation across the lifespan. The alignment is weakest during early childhood (approximately 6.9 years old) and is strongest in late adolescence (17.1 years old), emphasizing critical periods where genetic expression most influences neurophysiological individuality. The shaded area represents 95% CIs.

(B) Multivariate PLS analysis results.Left: significance (p values) of latent gene differentiation components, revealing significant covariance between cortical gene expression and neurophysiological differentiation across the lifespan, persisting through middle age. Points above the dashed line did not survive correction for multiple comparisons (false discovery rate [FDR]) or spatial autocorrelation.Middle: percent covariance explained by the latent components across different age groups. The variance explained remains relatively stable across age bins, suggesting a consistent gene-neurophysiology relationship throughout development and aging.Right: gene loadings show the relative contribution of neurophysiological frequency bands (theta, alpha, beta, and gamma) and genes to the covariance pattern. Strong consistency is observed across developmental stages as well as with loadings from prior independent analyses, demonstrating the stability of gene contributions to neurophysiological differentiation over time.

(C) Frequency band contributions across neurodevelopment. The graph depicts the relative contributions of neurophysiological frequency bands (theta [4–8 Hz]), alpha [8–13 Hz]), beta [13–30 Hz]), and gamma [30–50 Hz]) to gene-neurophysiology covariance. Positive loadings indicate alignment with the positive gene expression pattern, while negative loadings indicate alignment with the negative gene expression pattern (illustrated by the topographies on the far right). Theta band traits show a shift from negative alignment in early childhood to strong positive alignment in early adulthood. Alpha band contributions remain relatively stable across the lifespan. Beta band contributions reach their highest positive alignment in early adulthood, while gamma band contributions are strongest in adolescence. Gray dotted lines represent spline-interpolated trends for visualization and do not reflect model fits. Black outlines indicate the age bins with the strongest observed alignment (see main text).

First, using pseudo-neurophysiological traits derived from empty-room MEG data, we confirmed that environmental noise contributed minimally to differentiation (<5%; gray bars, Figure 1B).

Second, adding intracranial volume and head motion artifacts as nuisance covariates did not significantly alter the age-differentiability relationship in either cohort (Tables S6 and S7), and similar robustness was observed in Cam-CAN for head motion, cardiac, and ocular artifacts ($\beta = 0.01$, SE = 1.53×10^{-3}, 95% CI [0.00, 0.01], $p < 0.001$; Table S3).

Third, excluding participants above age 40 in SickKids did not change the observed effect ($\beta = 0.40$, SE = 0.05, 95% CI [0.30, 0.40], $p < 0.001$).

Fourth, in an artifact-matched subsample ($p = 0.26$ and $p = 0.13$ for intracranial volume and motion, respectively), children remained less differentiable than adults ($t = 4.50$, $p < 0.001$, BF = 1482), with salient-trait topographies closely matching those of the full sample (r = 0.77, pspin = 0.001; Figure S4).

Fifth, anatomical analyses indicated that cortical properties play a minimal role in spectral differentiation: child-child anatomical similarity was lower than adult-adult similarity ($t = -56.69$, $p < 0.01$), and there was no meaningful age-related linear relationship between anatomical and spectral other-similarity (Figure S5).

DISCUSSION

A growing body of research demonstrates that brain activity patterns, much like a fingerprint, are unique to each individual.[9–12] These neurophysiological traits are heritable,[19] correlate with inter-individual differences in cognition,[10,11,14] and manifest in disease processes.[15,16,60] However, the developmental trajectory

of these traits over the lifespan has been relatively unexplored. This study addressed a fundamental question: do individual neurophysiological traits become more distinctive across key developmental and aging stages?

Our findings reveal that individuals can be accurately differentiated based on patterns of periodic brain activity across the lifespan. However, the cortical regions most responsible for this differentiation shift with age. While neurophysiological traits are more homogeneous in childhood, sensorimotor regions become increasingly distinctive during the transition to adulthood. This shift is accompanied by a growing alignment between neurophysiological activity and gene expression, particularly involving genes related to ion transport and neurotransmission.

Periodic brain activity as a hallmark of individuality

This study underscores the centrality of periodic brain activity in distinguishing individuals across all age groups (Figure S8). This finding is consistent with prior research showing that periodic features remain robust markers of individuality, even in conditions such as Parkinson's disease, where aperiodic traits exhibit lower self-similarity within individuals.[16]

While periodic brain activity is characterized by stable repeating patterns of brain activity, the peak frequency and amplitude of brain rhythms are known to fluctuate within individuals throughout a brain recording. For example, alpha and beta band oscillations demonstrate transient bursts of increased activity at rest and during cognitive tasks.[69,70] Periodic brain activity, therefore, is not differentiable by definition; brain rhythms can fluctuate within individuals and can be similar to those of other individuals in a cohort, challenging participant differentiation.

Notably, children (ages 4–12) exhibited differentiation accuracy nearly equivalent to that of adolescents and adults despite the rapid and dynamic developmental changes occurring in childhood. This suggests that stable, individual-specific neurophysiological traits emerge early in life, even amid ongoing structural and functional maturation. The distinctiveness of children's periodic traits aligns with the development of major brain rhythms, including the transition from lower frequencies (3–7 Hz) to the alpha rhythm (8–13 Hz),[28–31] which stabilizes in late childhood, with a major developmental turning point around age 7.[71] Similar patterns are observed in somatomotor rhythms,[72] suggesting that neurophysiological individuality is present even as these rhythms continue to mature. These results challenge the assumption that younger brains are less individualized and highlight the resilience of periodic activity as a foundation for neurophysiological models.

Interestingly, while differentiation accuracy remained high across all age groups, other-similarity increased with age for periodic traits (Figure S8). Conversely, aperiodic traits became increasingly distinct with age (Figure S7). These opposing patterns tentatively suggest that periodic traits provide a stable marker of individuality, while aperiodic traits may evolve adaptively, possibly reflecting cortical plasticity and functional integration over the lifespan. Future research should explore the interplay between these components across cognitive and behavioral contexts.

We note that a growing body of evidence supports the close relationship between the arrhythmic component of brain activity and the balance of excitatory vs. inhibitory currents in local circuits.[27,37–39,73] More recent evidence suggests that arrhythmic brain activity tracks fluctuation in arousal during a biofeedback paradigm where participants learn to modulate their pupil size.[74] While children may show a more stereotyped topographic distribution of local excitatory vs. inhibitory activity, future research is needed to disambiguate these effects from other potential explanations, such as smaller head size.[75]

Gene expression and the molecular basis of neurophysiological differentiation

Our results shed light on how the alignment between cortical gene expression and individualized neurophysiological traits evolves across the lifespan (Figure 3). This alignment strengthens non-linearly with age, suggesting an increasing role of genetic factors in shaping brain individuality during neurodevelopment. We observed the strongest alignment between neurophysiological traits for participant differentiation and cortical gene expression in late adolescence (Figure 3). Genes related to ion transport and neurotransmission appear to drive this alignment, emphasizing the genetic underpinnings of individualized brain activity.

We observed that specific frequency bands contribute differentially to gene-neurophysiology alignment. Alpha band activity (8–13 Hz) consistently aligned with positive gene signatures across all ages, suggesting its enduring role in maintaining functional integrity. Conversely, theta band activity (4–8 Hz) showed an association with neurogenesis-related genes during early development, which diminished later in life. Beta band activity (13–30 Hz), associated with predictive coding and motor functions, demonstrated increasing alignment with positive gene signatures into adulthood. These findings illustrate the dynamic nature of frequency-specific molecular mechanisms underlying neurophysiological individuality. They may mirror the brain's changing functional demands across the lifespan. For instance, the increasing alignment of beta activity with genes involved in ion transport and neurotransmission in adulthood may reflect the greater reliance on sensorimotor networks for adaptive behavior.

Further, the distinct roles of positive and negative gene signatures highlight the complexity of brain individuality. While the positive signature consistently aligned with differentiable neurophysiological traits, the negative signature—linked to emotional processing[19,76]—showed greater variability across age groups. This suggests that different molecular pathways govern neurophysiological stability and flexibility, with positive genes supporting cognitive and motor functions and negative genes driving emotional regulation and responses to environmental stress.

The increasing role of sensorimotor regions in differentiation across the lifespan

Our findings show that the cortical regions most critical for individual differentiation shift over time, with sensorimotor regions—including visual and somatomotor cortex—playing an increasingly prominent role as individuals mature into adulthood (Figure 2A). This shift aligns with research indicating that sensorimotor areas gain importance in functional brain organization

as motor control and sensorimotor integration mature during neurodevelopment.[65]

Additionally, the alignment between cortical regions and functional gradients evolves with age. In childhood, characteristic brain regions align more closely with the visual-to-motor gradient, which plays a key role in early brain development. In adulthood, this alignment shifts toward the unimodal-to-transmodal gradient, reflecting the maturation of higher-order association cortices responsible for complex cognitive and emotional functions[24,25,47,77–80] (Figure 2B). We speculate that individual deviation from the group average functional gradient across the lifespan is critical for individual differentiation. Future studies utilizing FCs should clarify this interpretation.

This developmental shift underscores the role of sensorimotor regions in supporting predictive coding and inferential models, processes fundamental to cognition.[49–51,81–84] The increasing prominence of beta activity in these regions further highlights their genetic and functional specialization during development.[19]

While previous research using fMRI has argued for the central role of the frontoparietal network in inter-individual differentiation using functional connectivity, our study, in contrast, highlights the role of unimodal sensorimotor cortical regions in neurophysiological traits. These results are broadly aligned with previous work on brain fingerprinting using neural power spectra.[9,16,19] We previously observed that periodic brain activity in medial visual regions and the left somatomotor cortex were among the most differentiating features in healthy older adults (mean age of 61.98; see Figure S3 in da Silva Castanheira et al.[16]). We believe that the discrepancy between modalities underscores the distinct biological underpinnings of the hemodynamic response in fMRI and electrophysiological signals in MEG.[9,11,12,85] Indeed, the present findings and our previous work[19] have emphasized the alignment between neurophysiological traits and cortical gene expression gradients enriched for neuronal communication, particularly ion transport and neurotransmission. Our results thus provide insight into the potential biological mechanisms underlying neurophysiological individuality across development.

Neurophysiological differentiation in older adults: A compensatory mechanism?

Our findings also reveal greater differentiation in older adults based on broadband neurophysiological spectral features originating from sensorimotor regions, including motor and ventral-medial visual areas. When restricting our analyses exclusively to the Cam-CAN cohort, composed primarily of healthy older adults, we observed that the differentiation profile remained strongly aligned with the unimodal-to-transmodal functional gradient (Table S10). We therefore speculate that these effects likely reflect compensatory mechanisms for age-related sensory decline rather than disease-related changes, as older adults frequently exhibit reduced neural responsiveness to sensory stimuli.[86–88] Such compensatory processes may vary across individuals, potentially explaining the increased distinctiveness of sensorimotor activity in older adults. Importantly, sensory loss in aging is linked to elevated dementia,[89–94] suggesting that individual variability in sensory processing could serve as an early indicator of brain health.

Our findings appear to contrast with the "last in, first out" principle of neurodevelopment, where higher-order association areas, associated with complex cognitive functions, take the longest to develop and show the earliest reductions in cortical thickness.[24,25] One might predict that these transmodal association regions—which exhibit the largest and earliest signs of aging—would become more salient for individual differentiation. Yet, this interpretation rests on the assumption of a close link between structural changes and functional changes observed with neurophysiological traits, which our present findings (Figure S5) and previous work do not support.[19] In addition, we found that the increased other-similarity of neurophysiological traits in children could not be explained by increased anatomical similarity between participants. Future work should further explore the association between anatomy and neurophysiological traits.

In contrast, we observed weak evidence of a change in the topographic alignment between patterns of cortical gene expression previously associated with neurophysiological differentiation and neurophysiological traits. We interpret these findings to tentatively suggest that the genetic underpinnings of inter-individual diversity in neurophysiology in adulthood vary minimally across aging despite large shifts in early development (see subheading "The increasing role of sensorimotor regions in differentiation across the lifespan"). We argue that our findings, taken together with our previous work, provide scientists with a biologically grounded framework to understand the molecular origins of inter-individual diversity in neurophysiological signals captured throughout the lifespan. Animal models, we believe, will be paramount to assess the causal role of genes and their products in large-scale brain signaling.

Implications for health monitoring and brain-behavior relationships

Our findings underscore the importance of developmental stages in understanding neurophysiological differentiation and highlight the need for multi-omics data incorporating diverse socioeconomic, age, and geographical backgrounds.[95] Extending the concept of pediatric growth charts[20] to neurophysiological traits could enable approaches to monitoring brain health for tracking age-related brain changes. Extending this concept to neurophysiological traits could create opportunities for monitoring brain health and detecting deviations indicative of neurological or psychiatric conditions.[84]

The stability of both periodic and aperiodic traits has implications for understanding neurodevelopmental and neurodegenerative disorders. Delayed stabilization of these traits has been linked to atypical neurodevelopment, while greater stabilization correlates—albeit weakly—with better cognitive outcomes.[55] By establishing age-matched normative variants for neurophysiological differentiation, our study provides a foundation for further research of the diagnostic and prognostic utility of these traits in clinical contexts.

Prior work on brain fingerprinting in clinical populations, including mild cognitive impairment, dementia, and Parkinson's disease, has shown that, while individuals remain differentiable,[16,96] the specific regions driving differentiation differ. For example, individuals with mild cognitive impairment (MCI) with

β-amyloid positivity and patients with Parkinson's disease were best differentiated from activity in somatomotor regions.[16] Taken together with our present findings, we propose that increased differentiability in sensorimortor regions may reflect a continuum, from compensatory mechanisms in healthy aging to disease-related alterations, and may represent an important marker for health monitoring. Future studies are needed to test this hypothesis and validate these features as biomarkers in older populations.

Limitations of the study

While our study included a large, cross-sectional lifespan sample, longitudinal data are needed to provide a more accurate depiction of how neurophysiological traits evolve within individuals over time. Additionally, our gene expression analyses relied on an adult dataset, limiting insights into gene-neurophysiology alignment across developmental stages. Future research should prioritize data collection in infancy and early childhood, which remain underexplored. Advances in optically pumped magnetometers (OPMs) may facilitate neurophysiological data acquisition in younger populations.[97]

A strength—and limitation—of our approach lies in aggregating multiscale data from multiple research centers. While site effects cannot be fully ruled out, we repeated the analyses shown in Figures 2 and 3 using only Cam-CAN data and found qualitatively similar effects (Tables S11 and S13). We believe that future multi-site data sharing will be critical for assembling large, lifespan-spanning MEG cohorts for replication and extension of these findings.

Our findings demonstrate that periodic neurophysiological traits differentiate between individuals across all ages, yet the most salient features for participant differentiation evolve with increasing age. The most pronounced changes in neurophysiological traits occur below 13 years old and in older adults. These traits reflect dynamic interactions between genetic and environmental influences, with sensorimotor regions playing an increasingly prominent role in differentiation. By considering developmental and aging trajectories, future research can better capture the dynamic nature of the neurophysiological self and its implications for understanding individuality and brain health.

RESOURCE AVAILABILITY

Lead contact

Requests for further information and resources should be directed to and will be fulfilled by the corresponding author, Sylvain Baillet (sylvain.baillet@mcgill.ca).

Materials availability

This study did not generate new materials.

Data and code availability

- Data used in the preparation of this work are available through the Cam-CAN repository (https://Cam-CAN-archive.mrc-cbu.cam.ac.uk/). Data from the SickKids cohort will be available upon reasonable request from the lead contact. Cortical gene expression data were retrieved from two open source repositories and are available from the Allen Human Brain Atlas at https://human.brain-map.org/static/download and the BrainSpan database at https://www.brainspan.org/static/download.html.
- All codes for preprocessing, data analysis, and data visualization can be found on the project's GitHub site (https://github.com/jasondsc/brainfingerprintsR4ever).
- Any additional information required to reanalyze the data reported in this paper is available from the lead contact upon request.

ACKNOWLEDGMENTS

S.B. was supported by a Discovery grant from the Natural Sciences and Engineering Research Council of Canada (436355-13), the CIHR Canada Research Chair in Neural Dynamics of Brain Systems (CRC-2017-00311), the NIH (R01-EB026299-05), and the Canadian Institutes of Health Research (202503PJT-542788). This work was also supported by a doctoral fellowship from NSERC (JDSC) and by a CIHR Banting Postdoctoral Fellowship (BPF-186555 to A.I.W.) and the Canada Research Chairs (CRC-2023-00300 to A.I.W.) in Neurophysiology of Aging and Neurodegeneration. The SickKids MEG data collection was supported by CIHR funding to M.J.T. (MOP 106582, 137115, 142379, and 119541).

AUTHOR CONTRIBUTIONS

Conceptualization, J.d.S.C., A.I.W., M.J.T., and S.B.; data curation, J.d.S.C., M.J.T., and S.B.; methodology, J.d.S.C., A.I.W., and S.B.; software, J.d.S.C. and S.B.; visualization, J.d.S.C. and S.B.; resources, M.T. and S.B.; validation, J.d.S.C. and S.B.; formal analysis, J.d.S.C.; supervision, M.T. and S.B.; project administration, M.T. and S.B.; funding acquisition, M.T. and S.B.; writing – original draft, J.d.S.C. and S.B.; and writing – review and editing, J.d.S.C., A.I.W., M.T., and S.B.

DECLARATION OF INTERESTS

The authors declare no competing interests.

STAR★METHODS

Detailed methods are provided in the online version of this paper and include the following:

- KEY RESOURCES TABLE
- EXPERIMENTAL MODEL AND STUDY PARTICIPANT DETAILS
  - Participants: SickKids cohort
  - Participants: Cam-CAN cohort
  - Ethics
- METHOD DETAILS
  - Preprocessing of MEG data
  - Source modeling of MEG data
  - Neurophysiological traits
  - Gene expression
- QUANTIFICATION AND STATISTICAL ANALYSIS
  - Differentiation
  - Bootstrapping differentiation accuracy
  - Band-limited neurophysiological traits
  - Recording artifacts and differentiability
  - Empty-room differentiation
  - Aperiodic & periodic spectral parametrization
  - Relative contribution of features
  - Neuroanatomical similarity
  - Cortical functional hierarchy
  - Gene expression across the lifespan
  - Alignment to gene expression
  - Partial Least Squares analysis
  - Participant age permutation analyses

SUPPLEMENTAL INFORMATION

Supplemental information can be found online at https://doi.org/10.1016/j.celrep.2025.116657.

Received: March 18, 2025
Revised: September 25, 2025
Accepted: November 12, 2025
Published: December 11, 2025

REFERENCES

1. Dubois, J., and Adolphs, R. (2016). Building a Science of Individual Differences from fMRI. Trends Cogn. Sci. *20*, 425–443.
2. Van Horn, J.D., Grafton, S.T., and Miller, M.B. (2008). Individual Variability in Brain Activity: A Nuisance or an Opportunity? Brain Imaging Behav. *2*, 327–334.
3. Greene, A.S., Shen, X., Noble, S., Horien, C., Hahn, C.A., Arora, J., Tokoglu, F., Spann, M.N., Carrión, C.I., Barron, D.S., et al. (2022). Brain–phenotype models fail for individuals who defy sample stereotypes. Nature *609*, 109–118.
4. Avery, E.W., Yoo, K., Rosenberg, M.D., Greene, A.S., Gao, S., Na, D.L., Scheinost, D., Constable, T.R., and Chun, M.M. (2020). Distributed patterns of functional connectivity predict working memory performance in novel healthy and memory-impaired individuals. J. Cogn. Neurosci. *32*, 241–255.
5. Hsu, W.-T., Rosenberg, M.D., Scheinost, D., Constable, R.T., and Chun, M.M. (2018). Resting-state functional connectivity predicts neuroticism and extraversion in novel individuals. Soc. Cogn. Affect. Neurosci. *13*, 224–232.
6. Dhamala, E., Jamison, K.W., Jaywant, A., Dennis, S., and Kuceyeski, A. (2021). Distinct functional and structural connections predict crystallised and fluid cognition in healthy adults. Hum. Brain Mapp. *42*, 3102–3118.
7. Ooi, L.Q.R., Chen, J., Zhang, S., Kong, R., Tam, A., Li, J., Dhamala, E., Zhou, J.H., Holmes, A.J., and Yeo, B.T.T. (2022). Comparison of individualized behavioral predictions across anatomical, diffusion and functional connectivity MRI. Neuroimage *263*, 119636.
8. Kong, R., Tan, Y.R., Wulan, N., Ooi, L.Q.R., Farahibozorg, S.R., Harrison, S., Bijsterbosch, J.D., Bernhardt, B.C., Eickhoff, S., and Thomas Yeo, B.T. (2023). Comparison between gradients and parcellations for functional connectivity prediction of behavior. Neuroimage *273*, 120044.
9. da Silva Castanheira, J., Orozco Perez, H.D., Misic, B., and Baillet, S. (2021). Brief segments of neurophysiological activity enable individual differentiation. Nat. Commun. *12*, 5713.
10. Amico, E., and Goñi, J. (2018). The quest for identifiability in human functional connectomes. Sci. Rep. *8*, 8254.
11. Finn, E.S., Shen, X., Scheinost, D., Rosenberg, M.D., Huang, J., Chun, M.M., Papademetris, X., and Constable, R.T. (2015). Functional connectome fingerprinting: identifying individuals using patterns of brain connectivity. Nat. Neurosci. *18*, 1664–1671.
12. Sareen, E., Zahar, S., Ville, D.V.D., Gupta, A., Griffa, A., and Amico, E. (2021). Exploring MEG brain fingerprints: Evaluation, pitfalls, and interpretations. Neuroimage *240*, 118331.
13. Rosenberg, M.D., Finn, E.S., Scheinost, D., Constable, R.T., and Chun, M.M. (2017). Characterizing Attention with Predictive Network Models. Trends Cogn. Sci. *21*, 290–302.
14. Rosenberg, M.D., Scheinost, D., Greene, A.S., Avery, E.W., Kwon, Y.H., Finn, E.S., Ramani, R., Qiu, M., Constable, R.T., and Chun, M.M. (2020). Functional connectivity predicts changes in attention observed across minutes, days, and months. Proc. Natl. Acad. Sci. *117*, 3797–3807.
15. Troisi Lopez, E., Minino, R., Liparoti, M., Polverino, A., Romano, A., De Micco, R., Lucidi, F., Tessitore, A., Amico, E., Sorrentino, G., et al. (2023). Fading of brain network fingerprint in Parkinson's disease predicts motor clinical impairment. Hum. Brain Mapp. *44*, 1239–1250.
16. da Silva Castanheira, J., Wiesman, A.I., Hansen, J.Y., Misic, B., and Baillet, S.PREVENT-AD Research Group; Quebec Parkinson Network (2024). The neurophysiological brain-fingerprint of Parkinson's disease. EBioMedicine *105*, 105201.
17. Kaufmann, T., Alnæs, D., Doan, N.T., Brandt, C.L., Andreassen, O.A., and Westlye, L.T. (2017). Delayed stabilization and individualization in connectome development are related to psychiatric disorders. Nat. Neurosci. *20*, 513–515.
18. Kaufmann, T., Alnæs, D., Brandt, C.L., Bettella, F., Djurovic, S., Andreassen, O.A., and Westlye, L.T. (2018). Stability of the Brain Functional Connectome Fingerprint in Individuals With Schizophrenia. JAMA Psychiatry *75*, 749–751.
19. da Silva Castanheira, J., Poli, J., Hansen, J.Y., Misic, B., and Baillet, S. (2025). Genetic foundations of interindividual neurophysiological variability. Sci. Adv. *11*, eads7544.
20. Bethlehem, R.a.I., Seidlitz, J., White, S.R., Vogel, J.W., Anderson, K.M., Adamson, C., Adler, S., Alexopoulos, G.S., Anagnostou, E., Areces-Gonzalez, A., et al. (2022). Brain charts for the human lifespan. Nature *604*, 525–533.
21. Provencher, D., Hennebelle, M., Cunnane, S.C., Bérubé-Lauzière, Y., and Whittingstall, K. (2016). Cortical Thinning in Healthy Aging Correlates with Larger Motor-Evoked EEG Desynchronization. Front. Aging Neurosci. *8*, 63.
22. Salat, D.H., Buckner, R.L., Snyder, A.Z., Greve, D.N., Desikan, R.S.R., Busa, E., Morris, J.C., Dale, A.M., and Fischl, B. (2004). Thinning of the Cerebral Cortex in Aging. Cereb. Cortex *14*, 721–730.
23. Frangou, S., Modabbernia, A., Williams, S.C.R., Papachristou, E., Doucet, G.E., Agartz, I., Aghajani, M., Akudjedu, T.N., Albajes-Eizagirre, A., Alnaes, D., et al. (2022). Cortical thickness across the lifespan: Data from 17,075 healthy individuals aged 3-90 years. Hum. Brain Mapp. *43*, 431–451.
24. Sydnor, V.J., Larsen, B., Bassett, D.S., Alexander-Bloch, A., Fair, D.A., Liston, C., Mackey, A.P., Milham, M.P., Pines, A., Roalf, D.R., et al. (2021). Neurodevelopment of the association cortices: Patterns, mechanisms, and implications for psychopathology. Neuron *109*, 2820–2846.
25. Sydnor, V.J., Larsen, B., Seidlitz, J., Adebimpe, A., Alexander-Bloch, A.F., Bassett, D.S., Bertolero, M.A., Cieslak, M., Covitz, S., Fan, Y., et al. (2023). Intrinsic activity development unfolds along a sensorimotor–association cortical axis in youth. Nat. Neurosci. *26*, 638–649.
26. Donoghue, T., Haller, M., Peterson, E.J., Varma, P., Sebastian, P., Gao, R., Noto, T., Lara, A.H., Wallis, J.D., Knight, R.T., et al. (2020). Parameterizing neural power spectra into periodic and aperiodic components. Nat. Neurosci. *23*, 1655–1665.
27. Gao, R., Peterson, E.J., and Voytek, B. (2017). Inferring synaptic excitation/inhibition balance from field potentials. Neuroimage *158*, 70–78.
28. Saby, J.N., and Marshall, P.J. (2012). The Utility of EEG Band Power Analysis in the Study of Infancy and Early Childhood. Dev. Neuropsychol. *37*, 253–273.
29. Marshall, P.J., Bar-Haim, Y., and Fox, N.A. (2002). Development of the EEG from 5 months to 4 years of age. Clin. Neurophysiol. *113*, 1199–1208.
30. Rempe, M.P., Ott, L.R., Picci, G., Penhale, S.H., Christopher-Hayes, N.J., Lew, B.J., Petro, N.M., Embury, C.M., Schantell, M., Johnson, H.J., et al. (2023). Spontaneous cortical dynamics from the first years to the golden years. Proc. Natl. Acad. Sci. *120*, e2212776120.
31. Puligheddu, M., de Munck, J.C., Stam, C.J., Verbunt, J., de Jongh, A., van Dijk, B.W., and Marrosu, F. (2005). Age distribution of MEG spontaneous theta activity in healthy subjects. Brain Topogr. *17*, 165–175.
32. Merkin, A., Sghirripa, S., Graetz, L., Smith, A.E., Hordacre, B., Harris, R., Pitcher, J., Semmler, J., Rogasch, N.C., and Goldsworthy, M. (2023). Do age-related differences in aperiodic neural activity explain differences in resting EEG alpha? Neurobiol. Aging *121*, 78–87. https://doi.org/10.1016/j.neurobiolaging.2022.09.003.
33. Moretti, D.V., Paternicò, D., Binetti, G., Zanetti, O., and Frisoni, G.B. (2013). EEG upper/low alpha frequency power ratio relates to temporo-parietal

brain atrophy and memory performances in mild cognitive impairment. Front. Aging Neurosci. *5*, 63.

34. Babiloni, C., Binetti, G., Cassarino, A., Dal Forno, G., Del Percio, C., Ferreri, F., Ferri, R., Frisoni, G., Galderisi, S., Hirata, K., et al. (2006). Sources of cortical rhythms in adults during physiological aging: A multicentric EEG study. Hum. Brain Mapp. *27*, 162–172.
35. Scally, B., Burke, M.R., Bunce, D., and Delvenne, J.-F. (2018). Resting-state EEG power and connectivity are associated with alpha peak frequency slowing in healthy aging. Neurobiol. Aging *71*, 149–155.
36. Thuwal, K., Banerjee, A., and Roy, D. (2021). Aperiodic and Periodic Components of Ongoing Oscillatory Brain Dynamics Link Distinct Functional Aspects of Cognition across Adult Lifespan. eNeuro *8*, 0224-21.2021.
37. Maschke, C., Duclos, C., Owen, A.M., Jerbi, K., and Blain-Moraes, S. (2023). Aperiodic brain activity and response to anesthesia vary in disorders of consciousness. Neuroimage *275*, 120154.
38. Waschke, L., Donoghue, T., Fiedler, L., Smith, S., Garrett, D.D., Voytek, B., and Obleser, J. (2021). Modality-specific tracking of attention and sensory statistics in the human electrophysiological spectral exponent. eLife *10*, e70068.
39. Chini, M., Pfeffer, T., and Hanganu-Opatz, I. (2022). An increase of inhibition drives the developmental decorrelation of neural activity. eLife *11*, e78811.
40. Voytek, B., Kramer, M.A., Case, J., Lepage, K.Q., Tempesta, Z.R., Knight, R.T., and Gazzaley, A. (2015). Age-Related Changes in 1/f Neural Electrophysiological Noise. J. Neurosci. *35*, 13257–13265.
41. Voytek, B., and Knight, R.T. (2015). Dynamic Network Communication as a Unifying Neural Basis for Cognition, Development, Aging, and Disease. Biol. Psychiatry *77*, 1089–1097.
42. He, W., Donoghue, T., Sowman, P.F., Seymour, R.A., Brock, J., Crain, S., Voytek, B., and Hillebrand, A. (2019). Co-Increasing Neuronal Noise and Beta Power in the Developing Brain. Preprint at bioRxiv. https://doi.org/10.1101/839258.
43. Karalunas, S.L., Ostlund, B.D., Alperin, B.R., Figuracion, M., Gustafsson, H.C., Deming, E.M., Foti, D., Antovich, D., Dude, J., Nigg, J., and Sullivan, E. (2022). Electroencephalogram aperiodic power spectral slope can be reliably measured and predicts ADHD risk in early development. Dev. Psychobiol. *64*, e22228.
44. Schaworonkow, N., and Voytek, B. (2021). Longitudinal changes in aperiodic and periodic activity in electrophysiological recordings in the first seven months of life. Dev. Cogn. Neurosci. *47*, 100895.
45. Mills, K.L., Siegmund, K.D., Tamnes, C.K., Ferschmann, L., Wierenga, L.M., Bos, M.G.N., Luna, B., Li, C., and Herting, M.M. (2021). Inter-individual variability in structural brain development from late childhood to young adulthood. Neuroimage *242*, 118450.
46. Vanderwal, T., Eilbott, J., Kelly, C., Frew, S.R., Woodward, T.S., Milham, M.P., and Castellanos, F.X. (2021). Stability and similarity of the pediatric connectome as developmental measures. Neuroimage *226*, 117537.
47. Sato, J.R., Biazoli, C.E., Jr., Zugman, A., Pan, P.M., Bueno, A.P.A., Moura, L.M., Gadelha, A., Picon, F.A., Amaro, E., Jr., Salum, G.A., et al. (2021). Long-term stability of the cortical volumetric profile and the functional human connectome throughout childhood and adolescence. Eur. J. Neurosci. *54*, 6187–6201.
48. Dufford, A.J., Noble, S., Gao, S., and Scheinost, D. (2021). The instability of functional connectomes across the first year of life. Dev. Cogn. Neurosci. *51*, 101007.
49. Mollon, J., Knowles, E.E.M., Mathias, S.R., Gur, R., Peralta, J.M., Weiner, D.J., Robinson, E.B., Gur, R.E., Blangero, J., Almasy, L., and Glahn, D.C. (2021). Genetic influence on cognitive development between childhood and adulthood. Mol. Psychiatry *26*, 656–665.
50. Haworth, C.M.A., Wright, M.J., Luciano, M., Martin, N.G., de Geus, E.J.C., van Beijsterveldt, C.E.M., Bartels, M., Posthuma, D., Boomsma, D.I., Davis, O.S.P., et al. (2010). The heritability of general cognitive ability increases linearly from childhood to young adulthood. Mol. Psychiatry *15*, 1112–1120.
51. Briley, D.A., and Tucker-Drob, E.M. (2017). Comparing the Developmental Genetics of Cognition and Personality over the Lifespan. J. Pers. *85*, 51–64.
52. Wang, Q., Xu, Y., Zhao, T., Xu, Z., He, Y., and Liao, X. (2021). Individual Uniqueness in the Neonatal Functional Connectome. Cereb. Cortex *31*, 3701–3712.
53. Kardan, O., Kaplan, S., Wheelock, M.D., Feczko, E., Day, T.K.M., Miranda-Domínguez, Ó., Meyer, D., Eggebrecht, A.T., Moore, L.A., Sung, S., et al. (2022). Resting-state functional connectivity identifies individuals and predicts age in 8-to-26-month-olds. Dev. Cogn. Neurosci. *56*, 101123.
54. Demeter, D.V., Engelhardt, L.E., Mallett, R., Gordon, E.M., Nugiel, T., Harden, K.P., Tucker-Drob, E.M., Lewis-Peacock, J.A., and Church, J.A. (2020). Functional Connectivity Fingerprints at Rest Are Similar across Youths and Adults and Vary with Genetic Similarity. iScience *23*, 100801.
55. Fu, Z., Liu, J., Salman, M.S., Sui, J., and Calhoun, V.D. (2023). Functional connectivity uniqueness and variability? Linkages with cognitive and psychiatric problems in children. Nat. Ment. Health *1*, 956–970.
56. Graff, K., Tansey, R., Rai, S., Ip, A., Rohr, C., Dimond, D., Dewey, D., and Bray, S. (2022). Functional connectomes become more longitudinally self-stable, but not more distinct from others, across early childhood. Neuroimage *258*, 119367.
57. Jacobs, J., Hawco, C., Kobayashi, E., Boor, R., LeVan, P., Stephani, U., Siniatchkin, M., and Gotman, J. (2008). Variability of the hemodynamic response as a function of age and frequency of epileptic discharge in children with epilepsy. Neuroimage *40*, 601–614.
58. Issard, C., and Gervain, J. (2018). Variability of the hemodynamic response in infants: Influence of experimental design and stimulus complexity. Dev. Cogn. Neurosci. *33*, 182–193.
59. Gauthier, C.J., Madjar, C., Desjardins-Crépeau, L., Bellec, P., Bherer, L., and Hoge, R.D. (2013). Age dependence of hemodynamic response characteristics in human functional magnetic resonance imaging. Neurobiol. Aging *34*, 1469–1485.
60. Sorrentino, P., Rucco, R., Lardone, A., Liparoti, M., Troisi Lopez, E., Cavaliere, C., Soricelli, A., Jirsa, V., Sorrentino, G., and Amico, E. (2021). Clinical connectome fingerprints of cognitive decline. Neuroimage *238*, 118253.
61. Gao, M., Wong, C.H.Y., Huang, H., Shao, R., Huang, R., Chan, C.C.H., and Lee, T.M.C. (2020). Connectome-based models can predict processing speed in older adults. Neuroimage *223*, 117290.
62. Yu, J., and Fischer, N.L. (2022). Age-specificity and generalization of behavior-associated structural and functional networks and their relevance to behavioral domains. Hum. Brain Mapp. *43*, 2405–2418.
63. Taylor, J.R., Williams, N., Cusack, R., Auer, T., Shafto, M.A., Dixon, M., Tyler, L.K., Cam-Can, and Henson, R.N. (2017). The Cambridge Centre for Ageing and Neuroscience (Cam-CAN) data repository: Structural and functional MRI, MEG, and cognitive data from a cross-sectional adult lifespan sample. Neuroimage *144*, 262–269.
64. Margulies, D.S., Ghosh, S.S., Goulas, A., Falkiewicz, M., Huntenburg, J.M., Langs, G., Bezgin, G., Eickhoff, S.B., Castellanos, F.X., Petrides, M., et al. (2016). Situating the default-mode network along a principal gradient of macroscale cortical organization. Proc. Natl. Acad. Sci. *113*, 12574–12579.
65. Stoecklein, S., Hilgendorff, A., Li, M., Förster, K., Flemmer, A.W., Galiè, F., Wunderlich, S., Wang, D., Stein, S., Ehrhardt, H., et al. (2020). Variable functional connectivity architecture of the preterm human brain: Impact of developmental cortical expansion and maturation. Proc. Natl. Acad. Sci. *117*, 1201–1206.
66. Li, M., Santpere, G., Imamura Kawasawa, Y., Evgrafov, O.V., Gulden, F.O., Pochareddy, S., Sunkin, S.M., Li, Z., Shin, Y., Zhu, Y., et al.

(2018). Integrative functional genomic analysis of human brain development and neuropsychiatric risks. Science *362*, eaat7615.

67. Zhu, Y., Sousa, A.M.M., Gao, T., Skarica, M., Li, M., Santpere, G., Esteller-Cucala, P., Juan, D., Ferrández-Peral, L., Gulden, F.O., et al. (2018). Spatiotemporal transcriptomic divergence across human and macaque brain development. Science *362*, eaat8077.
68. Hawrylycz, M.J., Lein, E.S., Guillozet-Bongaarts, A.L., Shen, E.H., Ng, L., Miller, J.A., van de Lagemaat, L.N., Smith, K.A., Ebbert, A., Riley, Z.L., et al. (2012). An anatomically comprehensive atlas of the adult human brain transcriptome. Nature *489*, 391–399.
69. Lombardi, F., Herrmann, H.J., Parrino, L., Plenz, D., Scarpetta, S., Vaudano, A.E., de Arcangelis, L., and Shriki, O. (2023). Beyond pulsed inhibition: Alpha oscillations modulate attenuation and amplification of neural activity in the awake resting state. Cell Rep. *42*, 113162.
70. Liljefors, J., Almeida, R., Rane, G., Lundström, J.N., Herman, P., and Lundqvist, M. (2024). Distinct functions for beta and alpha bursts in gating of human working memory. Nat. Commun. *15*, 8950.
71. Cellier, D., Riddle, J., Petersen, I., and Hwang, K. (2021). The development of theta and alpha neural oscillations from ages 3 to 24 years. Dev. Cogn. Neurosci. *50*, 100969.
72. Berchicci, M., Zhang, T., Romero, L., Peters, A., Annett, R., Teuscher, U., Bertollo, M., Okada, Y., Stephen, J., and Comani, S. (2011). Development of Mu Rhythm in Infants and Preschool Children. Dev. Neurosci. *33*, 130–143.
73. Wiest, C., Torrecillos, F., Pogosyan, A., Bange, M., Muthuraman, M., Groppa, S., Hulse, N., Hasegawa, H., Ashkan, K., Baig, F., et al. (2023). The aperiodic exponent of subthalamic field potentials reflects excitation/inhibition balance in Parkinsonism. eLife *12*, e82467.
74. Weijs, M.L., Missura, S., Potok-Szybińska, W., Bächinger, M., Badii, B., Carro-Domínguez, M., Wenderoth, N., and Meissner, S.N. (2025). Modulating cortical excitability and cortical arousal by pupil self-regulation. Nat. Commun. *16*, 4552.
75. Quinn, A.J., Atkinson, L.Z., Gohil, C., Kohl, O., Pitt, J., Zich, C., Nobre, A.C., and Woolrich, M.W. (2024). The GLM-spectrum: A multilevel framework for spectrum analysis with covariate and confound modelling. Imaging Neurosci. *2*, 1–26.
76. Hansen, J.Y., Markello, R.D., Vogel, J.W., Seidlitz, J., Bzdok, D., and Misic, B. (2021). Mapping gene transcription and neurocognition across human neocortex. Nat. Hum. Behav. *5*, 1240–1250.
77. Batty, M., and Taylor, M.J. (2006). The development of emotional face processing during childhood. Dev. Sci. *9*, 207–220.
78. Mogadam, A., Keller, A.E., Taylor, M.J., Lerch, J.P., Anagnostou, E., and Pang, E.W. (2018). Mental flexibility: An MEG investigation in typically developing children. Brain Cogn. *120*, 58–66.
79. Taylor, M.J., and Pang, E.W. (1999). Developmental changes in early cognitive processes. Electroencephalogr. Clin. Neurophysiol. *49*, 145–153.
80. Cowan, N. (2014). Working Memory Underpins Cognitive Development, Learning, and Education. Educ. Psychol. Rev. *26*, 197–223.
81. Baillet, S. (2017). Magnetoencephalography for brain electrophysiology and imaging. Nat. Neurosci. *20*, 327–339.
82. Michalareas, G., Vezoli, J., van Pelt, S., Schoffelen, J.M., Kennedy, H., and Fries, P. (2016). Alpha-Beta and Gamma Rhythms Subserve Feedback and Feedforward Influences among Human Visual Cortical Areas. Neuron *89*, 384–397.
83. Morillon, B., and Baillet, S. (2017). Motor origin of temporal predictions in auditory attention. Proc. Natl. Acad. Sci. *114*, E8913–E8921.
84. Hipp, J.F., Engel, A.K., and Siegel, M. (2011). Oscillatory Synchronization in Large-Scale Cortical Networks Predicts Perception. Neuron *69*, 387–396.
85. Shafiei, G., Baillet, S., and Misic, B. (2022). Human electromagnetic and haemodynamic networks systematically converge in unimodal cortex and diverge in transmodal cortex. PLoS Biol. *20*, e3001735.
86. Takahashi, T., Cho, R.Y., Murata, T., Mizuno, T., Kikuchi, M., Mizukami, K., Kosaka, H., Takahashi, K., and Wada, Y. (2009). Age-related variation in EEG complexity to photic stimulation: A multiscale entropy analysis. Clin. Neurophysiol. *120*, 476–483.
87. Strömmer, J.M., Põldver, N., Waselius, T., Kirjavainen, V., Järveläinen, S., Björksten, S., Tarkka, I.M., and Astikainen, P. (2017). Automatic auditory and somatosensory brain responses in relation to cognitive abilities and physical fitness in older adults. Sci. Rep. *7*, 13699.
88. Stothart, G., and Kazanina, N. (2016). Auditory perception in the aging brain: the role of inhibition and facilitation in early processing. Neurobiol. Aging *47*, 23–34.
89. Chern, A., and Golub, J.S. (2019). Age-related Hearing Loss and Dementia. Alzheimer Dis. Assoc. Disord. *33*, 285–290.
90. Deal, J.A., Betz, J., Yaffe, K., Harris, T., Purchase-Helzner, E., Satterfield, S., Pratt, S., Govil, N., Simonsick, E.M., and Lin, F.R.; Health ABC Study Group (2017). Hearing Impairment and Incident Dementia and Cognitive Decline in Older Adults: The Health ABC Study. J. Gerontol. Ser. A *72*, 703–709.
91. Anang, J.B.M., Gagnon, J.F., Bertrand, J.A., Romenets, S.R., Latreille, V., Panisset, M., Montplaisir, J., and Postuma, R.B. (2014). Predictors of dementia in Parkinson disease. Neurology *83*, 1253–1260.
92. Dupuis, K., Pichora-Fuller, M.K., Chasteen, A.L., Marchuk, V., Singh, G., and Smith, S.L. (2015). Effects of hearing and vision impairments on the Montreal Cognitive Assessment. Aging Neuropsychol. Cogn. *22*, 413–437.
93. Gottfriedová, N., Kovalová, M., Mrázková, E., Machaczka, O., Koutná, V., Janout, V., and Janoutová, J. (2024). Assessment of sensory impairment in older adults with dementia. J. Otol. *19*, 220–226.
94. Salobrar-García, E., de Hoz, R., Ramírez, A.I., López-Cuenca, I., Rojas, P., Vazirani, R., Amarante, C., Yubero, R., Gil, P., Pinazo-Durán, M.D., et al. (2019). Changes in visual function and retinal structure in the progression of Alzheimer's disease. PLoS One *14*, e0220535.
95. Ricard, J.A., Parker, T.C., Dhamala, E., Kwasa, J., Allsop, A., and Holmes, A.J. (2023). Confronting racially exclusionary practices in the acquisition and analyses of neuroimaging data. Nat. Neurosci. *26*, 4–11.
96. Stampacchia, S., Asadi, S., Tomczyk, S., Ribaldi, F., Scheffler, M., Lövblad, K.O., Pievani, M., Fall, A.B., Preti, M.G., Unschuld, P.G., et al. (2024). Fingerprints of brain disease: connectome identifiability in Alzheimer's disease. Commun. Biol. *7*, 1169.
97. Brookes, M.J., Leggett, J., Rea, M., Hill, R.M., Holmes, N., Boto, E., and Bowtell, R. (2022). Magnetoencephalography with optically pumped magnetometers (OPM-MEG): the next generation of functional neuroimaging. Trends Neurosci. *45*, 621–634.
98. Miller, J.A., Ding, S.L., Sunkin, S.M., Smith, K.A., Ng, L., Szafer, A., Ebbert, A., Riley, Z.L., Royall, J.J., Aiona, K., et al. (2014). Transcriptional landscape of the prenatal human brain. Nature *508*, 199–206.
99. Tadel, F., Baillet, S., Mosher, J.C., Pantazis, D., and Leahy, R.M. (2011). Brainstorm: A User-Friendly Application for MEG/EEG Analysis. Comput. Intell. Neurosci. *2011*, 879716.
100. Markello, R.D., Arnatkeviciute, A., Poline, J.B., Fulcher, B.D., Fornito, A., and Misic, B. (2021). Standardizing workflows in imaging transcriptomics with the abagen toolbox. eLife *10*, e72129.
101. Fischl, B. (2012). FreeSurfer. Neuroimage *62*, 774–781.
102. Gross, J., Baillet, S., Barnes, G.R., Henson, R.N., Hillebrand, A., Jensen, O., Jerbi, K., Litvak, V., Maess, B., Oostenveld, R., et al. (2013). Good practice for conducting and reporting MEG research. Neuroimage *65*, 349–363.
103. Destrieux, C., Fischl, B., Dale, A., and Halgren, E. (2010). Automatic parcellation of human cortical gyri and sulci using standard anatomical nomenclature. Neuroimage *53*, 1–15.
104. R Core Team (2022). R: A Language and Environment for Statistical Computing (R Foundation for Statistical Computing).

105. Fulcher, B.D., Little, M.A., and Jones, N.S. (2013). Highly comparative time-series analysis: the empirical structure of time series and their methods. J. R. Soc. Interface *10*, 20130048.

106. Hawrylycz, M., Miller, J.A., Menon, V., Feng, D., Dolbeare, T., Guillozet-Bongaarts, A.L., Jegga, A.G., Aronow, B.J., Lee, C.K., Bernard, A., et al. (2015). Canonical genetic signatures of the adult human brain. Nat. Neurosci. *18*, 1832–1844.

107. Arnatkevičiūtė, A., Fulcher, B.D., and Fornito, A. (2019). A practical guide to linking brain-wide gene expression and neuroimaging data. Neuroimage *189*, 353–367.

108. Wilson, L.E., Castanheira, J.d.S., Kinder, B.L., and Baillet, S. (2024). Model selection for spectral parameterization. Preprint at bioRxiv. https://doi.org/10.1101/2024.08.01.606216.

109. Shrout, P.E., and Fleiss, J.L. (1979). Intraclass correlations: Uses in assessing rater reliability. Psychol. Bull. *86*, 420–428.

110. Markello, R.D., Hansen, J.Y., Liu, Z.Q., Bazinet, V., Shafiei, G., Suárez, L.E., Blostein, N., Seidlitz, J., Baillet, S., Satterthwaite, T.D., et al. (2022). Neuromaps: Structural and Functional Interpretation of Brain Maps. Preprint at bioRxiv. https://doi.org/10.1101/2022.01.06.475081.

111. Markello, R.D., and Misic, B. (2021). Comparing spatial null models for brain maps. Neuroimage *236*, 118052.

112. Váša, F., and Mišić, B. (2022). Null models in network neuroscience. Nat. Rev. Neurosci. *23*, 493–504.

113. Werling, D.M., Pochareddy, S., Choi, J., An, J.Y., Sheppard, B., Peng, M., Li, Z., Dastmalchi, C., Santpere, G., Sousa, A.M.M., et al. (2020). Whole-Genome and RNA Sequencing Reveal Variation and Transcriptomic Coordination in the Developing Human Prefrontal Cortex. Cell Rep. *31*, 107489.

114. McIntosh, A.R., and Mišić, B. (2013). Multivariate statistical analyses for neuroimaging data. Annu. Rev. Psychol. *64*, 499–525.

115. Krishnan, A., Williams, L.J., McIntosh, A.R., and Abdi, H. (2011). Partial Least Squares (PLS) methods for neuroimaging: a tutorial and review. Neuroimage *56*, 455–475.

STAR★METHODS

KEY RESOURCES TABLE

REAGENT or RESOURCE	SOURCE	IDENTIFIER
Open data		
CamCAN (open MEG dataset)	Taylor et al.[63]	https://Cam-CAN-archive.mrc-cbu.cam.ac.uk/
AHBA (Cortical gene expression data)	Hawrylycz et al.[68]	https://human.brain-map.org/static/download
BrainSpan (Cortical gene expression data)	Miller et al.[98]	https://www.brainspan.org/static/download.html.
Software and algorithms		
Brainstorm	Tadel et al.[99]	http://neuroimage.usc.edu/brainstorm/; RRID:SCR_001761
Abagen	Markello et al.[100]	https://abagen.readthedocs.io/en/stable/; RRID:SCR_023832
Freesurfer	Fischl[101]	https://surfer.nmr.mgh.harvard.edu/; RRID:SCR_001847
Python	Python	https://www.python.org; RRID:SCR_008394
R	R Core Team	https://www.r-project.org; RRID:SCR_001905
MATLAB	MATLAB	https://www.mathworks.com; RRID:SCR_001622

EXPERIMENTAL MODEL AND STUDY PARTICIPANT DETAILS

Participants: SickKids cohort

Data were collected from 401 healthy individuals aged 4–68 years (mean age = 20.79, SD = 14.14; 169 female; see Table S1 for demographics). Resting-state eyes-open magnetoencephalography (MEG) recordings lasted approximately 5 min and were acquired using a 151-channel whole-head CTF MEG system (Port Coquitlam, British Columbia, Canada) sampled at 600 Hz. Participants' head positions were continuously monitored throughout the recording using three Head-Position Indicator (HPI) coils to ensure consistent head localization. All participants also underwent structural T1-weighted MRI to inform MEG source modeling.

Participants: Cam-CAN cohort

Data were collected from 606 healthy individuals aged 18–89 years (mean age = 54.69, SD = 18.28; 299 female; see Table S2 for demographics) from the Cambridge Center for Aging and Neuroscience repository (Cam-CAN).[63] Each participant underwent a resting-state, eye-closed MEG recording using a 306-channel VectorView MEG system (MEGIN, Helsinki, Finland). The MEG system consisted of 102 magnetometers and 204 planar gradiometers, sampled sampling rate of 1 kHz with a 0.03–330 Hz bandpass filter. Resting-state recordings lasted approximately 8 min. Continuous monitoring of participants' head positions was performed using four HPI coils. Additionally, electrooculography (EOG) and electrocardiography (ECG) electrodes were used to capture ocular and cardiac artifacts for subsequent removal. T1-weighted MRI scans were also collected from all participants.

For demographic details of each dataset, see Tables S1 and S2.

Ethics

The procedures for the curation and analysis were reviewed and approved according to the institutional ethics policies of McGill University 's and the Montreal Neurological Institute's Research Ethics Boards (reference no. 22-11-021). Informed consent (assent when applicable) was obtained from all participants.

METHOD DETAILS

Preprocessing of MEG data

MEG data preprocessing was conducted using Brainstorm[99] (version dated 08-08-2023) in MATLAB R2021a (Mathworks Inc., Natick, Massachusetts, USA) adhering to good practice guidelines.[102] Preprocessing followed our prior work on MEG individual differentiation.[9,16,19]

Line noise artifacts at 50 Hz (Cam-CAN) and 60 Hz (SickKids), along with their first ten harmonics, were removed using a notch filter bank to ensure the removal of environmental and power-line interference. Additionally, an 88 Hz artifact characteristic of the Cam-CAN dataset was removed.

Slow-wave artifacts and DC offsets were mitigated using a high-pass finite impulse response filter with a 0.3-Hz cut-off frequency in both datasets.

Source modeling of MEG data

Brain source models were derived using individual participants' T1-weighted MRI scans to constrain MEG source mapping. MRI volumes were segmented and labeled automatically using FreeSurfer (version 7.3.2)[100]. The MRI data were co-registered with MEG recordings using approximately 100 digitized head points, when available.

We used Brainstorm's overlapping-spheres approach with default parameters for individual head models. Cortical source models were then computed with linearly-constrained minimum-variance (LCMV) beamforming (Brainstorm 2018 version for source estimation processes). MEG source orientations were constrained to be normal to the cortical surface. A grid of approximately 15,000 locations across the cortex was used for source modeling.

Neurophysiological traits

The power spectrum of MEG source time series at each cortical location was computed using the Welch method. This involves splitting the MEG recordings into 2-s windows with 50% overlap, computing the Fast Fourier Transform (FFT) for each window, and then averaging the power of the FFT coefficients across all windows to obtain a stable spectral estimate. Cortical surfaces were parcellated into 148 cortical regions using the Destrieux atlas.[103] We excluded the delta band (1–4 Hz) in the SickKids dataset due to the low signal-to-noise ratio, limiting analysis to frequencies between 4 and 150 Hz. For Cam-CAN, the analysis covered 1–150 Hz. The frequency resolution was set to 0.5 Hz, resulting in matrices of 148 cortical regions by 293 (SickKids) or 300 (Cam-CAN) frequency features for each participant. Spectral features were then exported to R (version 4.2.2)[104] for individual differentiation analyses.

Gene expression

We retrieved cortical gene expression data from six postmortem brains from the Allen Human Brain Atlas (AHBA; http://human.brain-map.org/).[68] Data were processed using the abagen Python package,[100] following our previously established pipeline,[19] with the exception of using the Destrieux atlas for cortical parcellation. We selected microarray probes with the highest differential stability to represent the expression of each gene, resulting in 20,232 genes included in our analysis.

Tissue samples were assigned to the nearest cortical region using a nonlinear registration method, focusing on minimizing misalignment across regions. Gene expression data were normalized across tissue samples and subjects,[105] and only genes with differential stability greater than 0.1 were retained, resulting in a final set of 9,278 genes. We retained only genes with a differential stability (DS) greater than 0.1, following prior work using the AHBA,[76,100,106,107] including our own previous analyses of neurophysiological trait heritability.[19] This threshold ensures consistency with established literature and maximizes comparability with previously derived cortical gene expression gradients.

We used previously defined sets of positive and negative genes, categorized based on their association with participant differentiation.[19] Genes positively correlated with differentiation were considered positive, while those negatively correlated were negative. After filtering for stability, we retained 2,076 positive genes and 2,219 negative genes. Cortical maps representing gene expression were generated to examine their alignment with the differentiable neurophysiological features observed across the lifespan.

QUANTIFICATION AND STATISTICAL ANALYSIS

Differentiation

Our differentiation method was adapted from previous work on neurophysiological differentiation.[9–11] Neurophysiological differentiation relied on differentiability of each participant across resting-state segments. We divided recordings into first and second halves to evaluate reproducibility and distinctiveness.

We obtained Pearson correlations between participant i's trait vector from the first segment (i.e., neurophysiological trait) and all trait vectors from the second segment. Correct differentiation occurred if participant i's self-similarity was greater than their other-similarity with any other participant in the cohort. Differentiation accuracy was then defined as the percentage of participants correctly differentiated according to this criterion.

For the SickKids cohort, we computed the differentiation accuracy in children (n = 148; 4–12 years old), adolescents (n = 57; 12–18 years old), adults (n = 196; 18+ years old), and the entire cohort (n = 401). We chose these age group boundaries to maximize the number of participants in the children and adult groups. To verify the robustness of our results, we slightly adjusted the definitions of the age groups and assessed their impact on differentiation accuracy. Details of this robustness check are presented in Figure S6.

A similar approach was used for the Cam-CAN cohort: young adults (18–45 years, n = 204), middle-aged adults (45–65 years, n = 194), older adults (65+ years, n = 208), and the entire cohort (n = 606).

Additionally, we computed a continuous differentiability score for each participant.[9] This score was calculated by z-scoring self-similarity relative to the mean and standard deviation of other-similarity scores. A high differentiability score indicated that a

participant's traits were more distinct from others in the cohort. We fitted the linear relationship using the lm() function in R to test the relationship between age and differentiability:

$$differentiability \sim \beta * age + intercept.$$

Bootstrapping differentiation accuracy

To assess reliability, we derived bootstrapped 95% confidence intervals for each differentiation accuracy. Participants were randomly sampled with replacement, subsampling 485 participants for the entire cohort and 175 for each age group in the Cam-CAN sample. For the SickKids Institute sample, 321 participants for the entire cohort were subsampled. Bootstrapping was repeated 1,000 times, and 2.5th and 97.5th percentiles of the resulting accuracy distribution were computed to provide confidence intervals, which reflect the empirical uncertainty.

The specific choice of the number of subsampled participants was made to balance the computational load with statistical power while ensuring consistency across the bootstrap samples. By defining our approach in this way, we aimed to maintain an adequate sample size that ensures robust estimation of the true differentiation accuracy for each cohort while accommodating practical considerations for data processing.

Band-limited neurophysiological traits

We replicated differentiation analyses using canonical electrophysiological frequency bands: delta (1–4 Hz), theta (4–8 Hz), alpha (8–13 Hz), beta (13–30 Hz), gamma (30–50 Hz), and high gamma (50–150 Hz). Delta band activity was excluded from SickKids analyses due to poor signal-to-noise ratio (SNR), limiting reliable differentiation.

Each canonical frequency band was subjected to the same differentiation analysis.

Recording artifacts and differentiability

We assessed the effect of common physiological artifacts on differentiability using regression models. Artifact levels were quantified using root-mean-square (RMS) values of ocular (VEOG, HEOG), cardiac (ECG), and head movement (HLU channels) artifacts across the MEG recording. Analyses were conducted separately for each dataset to account for specific differences.

We used regression models to determine whether physiological artifacts influenced individual differentiability, performing analyses separately in SickKids and Cam-CAN to account for cohort-specific differences. For Cam-CAN, head motion, cardiac, and ocular artifacts were included as nuisance covariates in linear regression models (see Tables S3). For SickKids, we assessed the effects of total intracranial volume (TIV) and head motion (Tables S6 and S7). To address the possibility of non-linear confounding, we repeated the regression models including quadratic terms for intracranial volume and log-transformed head motion. The results were consistent with the main analyses, with age-differentiability effects remaining significant after non-linear adjustment (see Table S7).

To further control for recording artifacts, we created a subgroup of participants who were matched on TIV and head motion artifact. This subsampling procedure yielded a sample size of 202 participants, 57 of whom were children below the age of 12. We then tested the robustness of our findings in this subsample: We examined whether i) we observed a similar age-differentiation effect with a two-sample permutation *t* test and ii) whether the most salient features for differentiating the artifact-matched sample of children were topographically aligned to those of the entire cohort of children. The findings of these analyses are presented in Figure S4.

Empty-room differentiation

To establish that individual differentiation was not driven by environmental or instrumental noise, we conducted empty-room differentiation using MEG recordings from the day of each participant's visit. For the SickKids dataset, only a single empty-room recording was available for the entire cohort. This recording was used to approximate the baseline noise level. Empty-room data were pre-processed similarly to participant data, except for physiological artifact removal. These recordings were used to generate pseudo neurophysiological traits. Differentiation accuracy using these pseudo-traits served as a baseline performance measure, ensuring that results were not due to noise.[9] The results of this analysis are plotted in Figure 1 (i.e., the gray bars).

Aperiodic & periodic spectral parametrization

To assess the contribution of aperiodic neurophysiological activity to individual differentiability, we parametrized the participants' MEG source power spectra using the ms-specparam tool in Brainstorm.[99,108] We extracted the aperiodic background components from periodic oscillatory peaks in each source signal spectrum.

For the SickKids dataset, the frequency range for analysis was set between 4 and 50 Hz, while for the Cam-CAN dataset, it was set between 1 and 40 Hz. The peak width limits differed slightly, with the SickKids dataset having limits between 1 and 8 Hz, and the Cam-CAN dataset between 0.5 and 12 Hz. We specified a maximum of six peaks per spectrum, with a minimum peak amplitude of 1 arbitrary unit (a.u.). The peak detection threshold was set at two standard deviations above the mean, while the proximity threshold, determining how close detected peaks could be, was set at 0.75 standard deviations. The aperiodic component was modeled using a fixed mode to ensure consistency across participants.

These hyperparameters for spectral parametrization were determined based on visual inspection of the spectra, to ensure that the model captured the relevant spectral features while minimizing the risk of overfitting or misinterpretation.

Following spectral parametrization, the (a)periodic components were used to derive neurophysiological traits defined from (a)periodic spectral features. The differentiation procedure was then carried out using the previously described approach, where we evaluated how well participants could be differentiated based solely on the aperiodic vs. periodic spectral components fits of their cortical neurophysiological activity.

Relative contribution of features

We calculated intraclass correlations (ICC) using a one-way random effects model to evaluate the contribution of each feature (frequency x cortical region) to participant differentiation.[9,10,109] This approach follows from previous brain-fingerprinting work.[9,10,16,19] ICC quantifies the ratio of within-participant to between-participant variance of neurophysiological traits, where high ICC values indicate that a specific neurophysiological feature is consistently similar within participants across repeated measures while being distinct across different participants. Therefore, features with high ICC values contribute most significantly to participant differentiation.

To generate the brain maps presented in Figures 2 and S11, we initially averaged ICC values within each canonical frequency band (e.g., theta, alpha, beta, gamma). Following this, we averaged across the resulting frequency band maps to derive a broadband saliency topography. This two-step averaging was performed to ensure that each frequency band had an equal influence on the overall saliency map, independent of differences in frequency band definitions (e.g., the theta bandwidth spans 4 Hz, while gamma covers at least 20 Hz).

We pooled data from both the SickKids and Cam-CAN datasets to obtain a comprehensive representation of how feature saliency changes across the lifespan. Participants were ordered by ascending age, and we used a sliding window approach to calculate ICC values for each age group. Specifically, we selected a moving window of 100 participants with 75% overlap between consecutive windows, which resulted in 37 ICC maps representing increasing age bins. Note, we tested the robustness of our results using a moving window of 50 participants with 50% overlap (see Tables S11 and S13). This method allowed us to capture the gradual changes in the contribution of different cortical regions and frequency bands to individual differentiation as participants age. The results of this analysis are visualized in Figure 2A, which illustrates the shifting topographic features that characterize individualized neurophysiology across the lifespan.

Neuroanatomical similarity

To ensure that increased other-similarity observed in children was not due to anatomical features, we conducted additional analyses incorporating neuroanatomical data. Specifically, we extracted nine anatomical features for each cortical region defined by the Destrieux atlas,[103] which were provided by the FreeSurfer segmentation process.[101] These features included metrics such as cortical thickness, surface area, and volume.

We used these anatomical features to construct an anatomical similarity matrix that quantified the similarity between each pair of participants based on their anatomical characteristics. This matrix was derived by computing Pearson correlations between the anatomical features of all possible participant pairs.

We then evaluated whether this anatomical similarity could explain the observed other-similarity in neurophysiological traits, particularly the greater similarity observed in children. To do this, we computed the linear relationship between participant-pair anatomical similarity and neurophysiological similarity across all pairs.

Cortical functional hierarchy

We assessed whether the pattern of cortical regions contributing most to differentiation increasingly aligned with the functional organization of the cortex with age. Specifically, we evaluated their correspondence with the unimodal-to-transmodal gradient, which represents the functional hierarchy of cortical regions from primary sensory to higher-order association areas.[64]

To evaluate this correspondence, we computed the spatial alignment between the ICC maps (derived from the sliding window approach, see above) and the unimodal-to-transmodal functional gradient obtained using the neuromaps toolbox.[110] This alignment was quantified using Pearson correlation for each age bin, capturing the degree to which regions involved in individual differentiation align with the functional gradient of the cortex.

We further examined whether this alignment changed non-linearly across the lifespan by fitting a third-order polynomial model to capture potential trends. To test the robustness of observed changes, we used 1,000 autocorrelation-preserving permutation tests using the Hungarian spin method. These permutation tests generated spin-based resampling of cortical maps to assess statistical significance while preserving spatial autocorrelation.[111,112]

For each spin permutation, we recalculated the alignment between the permuted functional gradient map and the ICC maps, fitting a third-order polynomial to the resulting alignment data. We then computed the permuted p-value by comparing the observed third-order polynomial beta-coefficients with those obtained from the permuted data, allowing us to assess the statistical significance of the observed alignment patterns.

We also evaluated the alignment between the pattern of cortical regions contributing the most to differentiation and the visual-to-motor functional gradient,[64] hypothesized to be more relevant for early brain development. The same procedures for spatial alignment and permutation testing were applied (see Figure 2A).

Gene expression across the lifespan

To evaluate the stability of positive and negative gene signatures identified in our previous work,[19] we analyzed gene expression data across developmental stages, from 8 post-conception weeks to 40 years of age, using data from 16 cortical regions obtained from the BrainSpan Atlas.[98] Gene expression data were grouped into five life stages[19,76,113]: fetal (8–37 post-conception weeks), infant (4 months–1 year), child (2–8 years), adolescent (11–19 years), and adult (21–40 years). For each developmental stage, we computed the average expression levels of the positive and negative gene sets across the cortical regions.

To assess the stability of these spatial gene expression patterns across different life stages, we calculated Pearson correlations between the cortical expression patterns of all pairs of life stages. This resulted in a symmetric topographic similarity matrix for the positive and negative gene sets separately (Figure S12).

Alignment to gene expression

To investigate whether the alignment between the pattern of cortical regions that contribute to differentiation and cortical gene expression changed across the lifespan, we computed the spatial alignment between the ICC maps and the positive gene expression signature. This alignment was assessed using Pearson correlations to quantify the similarity between the spatial distribution of differentiable features and gene expression patterns.

We used a sliding window approach across different age bins to examine changes in this alignment throughout the lifespan. This allowed us to explore how the developmental progression of neurophysiological features aligns with the expression of genetic systems across the cortex.

Partial Least Squares analysis

To further explore the alignment between cortical gene expression and neurophysiological traits, we conducted a Partial Least Squares (PLS) analysis for each age group. This multivariate analysis was used to relate the most differentiable cortical regions (as quantified by ICC values) at each age bin (Figure 2A) to cortical gene expression patterns obtained from the Allen Human Brain Atlas.[68]

For each age bin, we constructed two data matrices: one containing distinctive neurophysiological traits (represented by the ICC values) and another containing the cortical gene expression data. The traits matrix had four columns (each representing a frequency band) and 148 rows, corresponding to the cortical regions of the Destrieux atlas. The gene expression matrix had 9,278 columns (representing genes) and 148 rows (representing cortical regions).

To ensure comparability, we z-scored the columns of each matrix before applying Singular Value Decomposition (SVD) to the cross-covariance matrix between the neurophysiological and gene matrices. The resulting latent components provided insight into the covariance structure between the neurophysiological features and gene expression across age bins:

$$(Y'X)' = USV'.$$

Here, U is a 9,278 by 4 orthonormal matrix, and V is a 4 by 4 orthonormal matrix, with each column representing a latent component of the covariance between neurophysiological traits and gene expression. This decomposition was repeated for each age group using a sliding window approach, as described above. We reported the percentage of covariance explained by each latent component, giving insight into the relationships between neurophysiological features and genetic expression across age bins.[114,115]

To assess the significance of the latent components, we conducted 1,000 spatial autocorrelation-preserving permutation tests using the Hungarian spin method (detailed above). We generated null distributions of singular values from these permutations to compute empirical p-values, which were corrected for multiple comparisons using False Discovery Rate (FDR) correction, as implemented in MATLAB.

To determine the contribution of individual genes and frequency bands to the observed patterns of covariance, we computed Pearson correlations between each variable's spatial distribution over the cortex (i.e., gene expression and ICC values) and the opposing PLS brain score pattern.[19,76] These loadings are bounded between −1 and 1, facilitating intuitive interpretation—large absolute loadings indicate strong contributions to the latent component of covariance.

Lastly, to evaluate the consistency of gene contributions across the lifespan, we assessed the similarity between the gene loadings derived from each age bin with our previously reported gene loadings from an independent PLS analysis using MEG data from the Human Connectome Project.[19] This was done using Pearson correlations (Figure 3B, right panel), which provided insight into the stability of the genetic signature governing differentiable neurophysiological activity throughout development and aging.

Participant age permutation analyses

To assess the robustness of the non-linear neurodevelopmental effects presented in Figures 2 and 3, we permuted the association between each participant's neurophysiological trait and their age 500 times. Each permuted dataset was analyzed using the same sliding-window approach described in Relative Contribution of Neurophysiological Traits. A third-order polynomial regression model was then fit to the resulting alignment values, and the true beta coefficients were compared to those from the permutations to derive a p-value.